Phenomenological theory of the superconductivity phase diagram of $U_{1-x}Th_xBe_{13}$

Manfred Sigrist and T. M. Rice
Theoretische Physik, Eidgenössische Technische Hochschule-Hönggerberg, 8093 Zürich, Switzerland
(Received 15 March 1988; revised manuscript received 12 August 1988)

Possible phenomenological theories to describe the phase diagram of $U_{1-x}Th_xBe_{13}$ based on a crossing of two different types of anisotropic superconductivity at $x \approx 0.018$ are examined. In this description the second transition for $x > 0.018$ is interpreted as a further superconducting transition. It is shown that measurements of the critical magnetic field support this assumption. The effects of uniform pressure and the specific-heat measurements are qualitatively in a good agreement with these theories. The large peak in the ultrasonic attenuation in the low-temperature phase in the region $x > 0.018$ is explained by a dissipative domain-wall motion, induced by the sound wave, which in this case couples in both [001] and [111] directions. The theory predicts nonunitary superconducting states below the second phase transition. Such states have a finite local spin polarization in each unit cell, which leads to an explanation of zero-field relaxation rate data in muon-spin-rotation experiments.

I. INTRODUCTION

Since the discovery of superconductivity in the heavy-electron metals, $CeCu_2Si_2$ (Ref. 1), UBe_{13} (Ref. 2), and UPt_3 (Ref. 3), there has been a continuous effort to establish the symmetry of the superconducting states (for recent reviews see Refs. 4 and 5). By using group-theoretical methods, a complete classification of the possible symmetries of the superconducting phases has been obtained by several groups under the the assumption that the order parameter is constructed only from basis functions belonging to a single representation.[6-10] The discovery of a complex phase diagram when Th was substituted for U in UBe_{13} has led to a special interest in this alloy system.[11] Several models have been proposed, but at present there is no consensus on the interpretation of all experiments. This alloy series, $U_{1-x}Th_xBe_{13}$, will be the focus of this paper. Our aim will be to seek a consistent explanation of all outstanding experimental data within a single phenomenological model.

First, we briefly recapitulate the key experimental results: (a) specific-heat experiments by Ott *et al.* discovered a sharp minimum in the normal-superconducting transition temperature $T_c(x)$ at $x = x_0$ (≈ 0.018) and a further second-order transition at T_{c2} ($< T_c$) for values of $x > x_0$ leading to a phase diagram of the form shown in Figs. 1(a) (Ref. 12), (b) Batlogg *et al.* found a pronounced peak in the ultrasonic attenuation for longitudinal sound propagated along a [100] direction at $T = T_{c2}$ and an increased level of attenuation for $T < T_c$ (by contrast, at $T = T_c$ there is only a very small anomaly for $x > x_0$) (Ref. 13). Later experiments by Bishop *et al.* showed a similar (but somewhat weaker) behavior for longitudinal sound along [111] directions[14] (c) Lambert *et al.* found a marked difference in the pressure dependence of T_c for samples for $x < x_0$ and samples with values of $x > x_0$ (Ref. 15) (d) Rauchschwalbe *et al.* found a pronounced anomaly in $H_{c1}(T)$ at $T = T_{c2}$ with a marked increase in H_{c1} for $T < T_{c2}$ (Ref. 16) and lastly (e) Heffner *et al.* found a marked increase in the zero-field μSR linewidth as T decreased below T_{c2} in a sample with $x \approx 0.033$ ($> x_0$) (Ref. 17).

There are several theoretical proposals to explain part or all of these results. In the first proposal, Joynt, Rice, and Ueda proposed that the anomaly in $T_c(x)$ arose because two different representations crossed so that the superconducting states for $x < x_0$ and $x > x_0$ belonged to different symmetries.[18] Further, they proposed that for $x > x_0$, the second transition at T_{c2} was between two different combinations of basis functions derived from the same representation. From this latter proposal they predicted that the anomaly in ultrasonic attenuation, which they assumed to be due to a coupling to domain walls between different superconducting domains, should be absent for [111] longitudinal waves—a prediction which was disproved in later experiments by Bishop *et al.*[14] In the original ultrasonic study, Batlogg *et al.* proposed that the anomaly at T_c was analogous to that observed at itinerant antiferromagnetic transitions, and that transition was to an antiferromagnetic state.[13] The subsequent μSR experiments by Heffner *et al.* have been taken as support for this proposal.[17] In addition, a microscopic model of the coexistence of antiferromagnetism and superconductivity was examined by Machida and Kato.[19] However, it is not clear why $T_c(x)$ is anomalous in this model and the H_{c1} measurements of Rauchschwalbe *et al.* pointed to an essential change in the superconductivity and even an increase in the superconducting condensation energy. This led, then, to the proposal by Rauchschwalbe *et al.* that there were two essentially decoupled parts of the Fermi surface with one going superconducting at T_c and the other at T_{c2} (Refs. 16 and 20). However, on microscopic grounds this is not so easy to understand unless there is a symmetry change at T_{c2}. Very recently, Kumar and Wolfle have examined a simplified model with crossing s- and d-wave superconductivity.[21]

In this work, we wish to return the proposal of Joynt *et al.* of two crossing representations and examine within a Ginzburg-Landau theory the form of possible phase diagrams for values of x near to x_0. There are very many possibilities both as regards the symmetries that cross and the many unknown parameters in the terms in the Ginzburg-Landau expansion that couple two representations. A complete investigation would be very tedious and have little use. Instead we will concentrate on the simplest examples which are compatible with all the experiments and are most tractable analytically. Even so, there are many possibilities, and in the end we will only be able to conclude that this theory can consistently explain all results but does not uniquely identify the symmetries involved. Our proposal, then, is that the superconducting state at $T<T_c$ belongs to single but different representations in the regions $x<x_0$ and $x>x_0$, and that the transition at T_{c2} is to a state formed by a combination of both representations. It is on this latter point where we differ from the proposal of Joynt *et al.* The examination of this proposal is the purpose of this paper.

The outline of the paper is as follows. We begin with a summary of the standard group theory and then discuss the pressure experiments of Lambert *et al.* The form of the Ginzburg-Landau expansion when there is more than one relevant representation is discussed in Sec. III. Then, in Sec. IV we begin the study of crossing representations with the case (Γ_1,Γ_3), and, subsequently, the cases (Γ_1,Γ_5) or (Γ_1,Γ_4). In Sec. V the crossing of two higher dimensional representations is treated and some of the possible phase diagrams are presented in Sec. VI. Then, we discuss, in turn, the specific-heat experiments (Sec. VII), the ultrasonic attenuation experiments (Sec. VIII), H_{c1} experiments (Sec. IX) and lastly, μSR experiments (Sec. X). Finally, we summarize our results in the last section (Sec. XI).

II. THE CROSSING OF TWO REPRESENTATIONS

We begin with a brief recapitulation of the standard results.[6–10] The gap function

$$\hat{\Delta}_{\alpha\beta}(\mathbf{k})=-\sum_{\mathbf{k},\gamma\gamma'}V_{\alpha\beta\gamma\gamma'}(\mathbf{k},\mathbf{k}')\langle c_{\mathbf{k}\gamma}c_{-\mathbf{k}\gamma'}\rangle$$

is a 2×2 matrix [$c^{+}_{\mathbf{k}\alpha}$ ($c_{\mathbf{k}\alpha}$) is the creation-(annihilation) operator of a Bloch spinor] and $V_{\alpha\beta\gamma\gamma'}(\mathbf{k},\mathbf{k}')$ is a matrix element of the pairing interaction] and with the standard notation we describe an odd-parity state (p wave) by a vector $\mathbf{d}(\mathbf{k})$, and an even-parity (s wave or d wave) by a scalar $\psi(\mathbf{k})$:

$$\hat{\Delta}(\mathbf{k})=i\sum_{j=x,y,z}d^{j}(\mathbf{k})\hat{\sigma}^{j}\hat{\sigma}^{y}\ , \tag{1a}$$

$$\hat{\Delta}(\mathbf{k})=i\psi(\mathbf{k})\hat{\sigma}^{y}\ , \tag{1b}$$

where $\hat{\sigma}^{j}$ denotes the Pauli-spin matrices. Note we have included spin-orbit coupling derived terms in the pairing interaction. In the odd-parity case there is a set of orthonormal basis functions $\mathbf{d}(\Gamma,m,\mathbf{k})$ belong to each irreducible representation Γ of the cubic point group O: Γ_1 (one-dimensional), Γ_3 (two-dimensional), Γ_4 and Γ_5 (three-dimensional) (see Table I).[7] They can be derived as the components of the decomposition of the product $\Gamma_4\otimes\Gamma_4$, where Γ_4 is the vector-and spin-1 representation of O. Similarly, for the even-parity case the representation Γ_3 and Γ_5 supply an orthonormal basis $\psi(\Gamma,j;\mathbf{k})$ for the d-wave states (see Table I). An arbitrary gap matrix can be expanded by using the forms

$$\mathbf{d}(\mathbf{k})=\sum_{\Gamma,m}\lambda(\Gamma,m)\mathbf{d}(\Gamma,m;\mathbf{k})\ , \tag{2a}$$

$$\psi(\mathbf{k})=\sum_{\Gamma,m}\lambda(\Gamma,m)\psi(\Gamma,m;\mathbf{k})\ . \tag{2b}$$

The coefficients $\lambda(\Gamma,m)$ transform under the elements of O like the basis function of Γ. We can use these $\lambda(\Gamma,m)$ as order parameters in a Ginzburg-Landau expansion of the free energy F. In the standard approach we assume that only one Γ_i of the previously mentioned irreducible representations is relevant for the phase transition, namely that for which the transition temperature,

TABLE I. Upper part: Basis function $\mathbf{d}(\Gamma,m;\mathbf{k})$ for p-wave pairing with spin-orbit coupling. The momentum space $\{k_x,k_y,k_z\}$ and the spin space $\{\hat{\mathbf{x}},\hat{\mathbf{y}},\hat{\mathbf{z}}\}$ are connected in the product $\Gamma_4\otimes\Gamma_4=\Gamma_1\oplus\Gamma_3\oplus\Gamma_4\oplus\Gamma_5$ of the underlain cubic symmetry (point group O). $\hat{l}$ denotes a unit vector in l direction. lower part: Basis functions $\psi(\Gamma,m;\mathbf{k})$ for d-wave pairing. In the cubic symmetry d-wave states belong to the two irreducible representations Γ_3 and Γ_5 of the point group O.

Γ	$\mathbf{d}(\Gamma,m,;\mathbf{k})$
Γ_1	$\frac{1}{\sqrt{3}}(\hat{\mathbf{x}}k_x+\hat{\mathbf{y}}k_y+\hat{\mathbf{z}}k_z)$
Γ_3	$\frac{1}{\sqrt{6}}(2\hat{\mathbf{z}}k_z-\hat{\mathbf{x}}k_x-\hat{\mathbf{y}}k_y)$
	$\frac{1}{\sqrt{2}}(\hat{\mathbf{x}}k_x-\hat{\mathbf{y}}k_y)$
Γ_4	$\frac{1}{\sqrt{2}}(\hat{\mathbf{y}}k_z-\hat{\mathbf{z}}k_y)$
	$\frac{1}{\sqrt{2}}(\hat{\mathbf{z}}k_x-\hat{\mathbf{x}}k_z)$
	$\frac{1}{\sqrt{2}}(\hat{\mathbf{x}}k_y-\hat{\mathbf{y}}k_x)$
Γ_5	$\frac{1}{\sqrt{2}}(\hat{\mathbf{y}}k_z+\hat{\mathbf{z}}k_y)$
	$\frac{1}{\sqrt{2}}(\hat{\mathbf{z}}k_x+\hat{\mathbf{x}}k_z)$
	$\frac{1}{\sqrt{2}}(\hat{\mathbf{x}}k_y+\hat{\mathbf{y}}k_x)$

Γ	$\psi(\Gamma,m;\mathbf{k})$
Γ_3	$\frac{1}{\sqrt{6}}(2k_z^2-k_x^2-k_y^2)$
	$\frac{1}{\sqrt{2}}(k_x^2-k_y^2)$
Γ_5	$\sqrt{2}k_yk_z$
	$\sqrt{2}k_zk_x$
	$\sqrt{2}k_xk_y$

TABLE II. Invariant fourth-order terms in the GL expansion corresponding to a single representation Γ. The order parameters are successively numerated through all representations ($\lambda_i; i=1,\ldots,9$). The coefficients β_1, β_i, η_i, and η_i' are not determined by symmetry arguments and, therefore, are regarded as arbitrary eligible.

Γ	$f(\lambda^4)$
Γ_1	$\beta\lvert\lambda_1\rvert^4$
Γ_3	$\beta_1(\lvert\lambda_2\rvert^2+\lvert\lambda_3\rvert^2)^2+\beta_2(\lambda_2^*\lambda_3-\lambda_2\lambda_3^*)^2$
Γ_4	$\eta_1(\lvert\boldsymbol{\lambda}\rvert^2)^2+\eta_2\lvert\boldsymbol{\lambda}^2\rvert^2+\eta_3(\lvert\lambda_4\rvert^2\lvert\lambda_5\rvert^2+\lvert\lambda_5\rvert^2\lvert\lambda_6\rvert^2+\lvert\lambda_6\rvert^2\lvert\lambda_4\rvert^2)$
Γ_5	$\eta_1'(\lvert\boldsymbol{\lambda}\rvert^2)^2+\eta_2'\lvert\boldsymbol{\lambda}^2\rvert^2+\eta_3'(\lvert\lambda_7\rvert^2\lvert\lambda_8\rvert^2+\lvert\lambda_8\rvert^2\lvert\lambda_9\rvert^2+\lvert\lambda_9\rvert^2\lvert\lambda_7\rvert^2)$

$T_c(\Gamma_i)$, is the largest among the $T_c(\Gamma)$.

The free energy per unit volume can be written in a Ginzburg-Landau expansion as

$$F_\Gamma=\alpha\left[A(T)\sum_m \lvert\lambda(\Gamma,m)\rvert^2+f_\Gamma(\lambda^4)\right], \tag{3}$$

with $A(T)=T/T_c-1$, and α is a constant of order $T_c^2N(E_F)$ [$N(E_F)$ is the density of states at the Fermi energy]. The fourth-order terms written as $f_\Gamma(\lambda^4)$ contain all combinations which are invariant under all symmetries of the system (Table II). The determination of the minimum of $F_\Gamma(\lambda)$ for every Γ leads to a complete classification of the possible superconducting phases within the single representation restriction.

Returning to the $U_{1-x}Th_xBe_{13}$ alloys following Joynt *et al.*, we wish to explain the nonmonotonic behavior of the critical temperature by a crossing of the values of $T_c(\Gamma,x)$ of two irreducible representations Γ and Γ' at x_0. For $x<x_0$ (region I) Γ is the relevant representation for the superconductivity ($T_c(\Gamma,x)>T_c(\Gamma',x)$), but for $x>x_0$, (region II), Γ' becomes relevant ($T_c(\Gamma',x)>T_c(\Gamma,x)$) [see Fig. 1(b)]. Therefore, two different types of supeconductivity appear in these two regions of Th concentration.

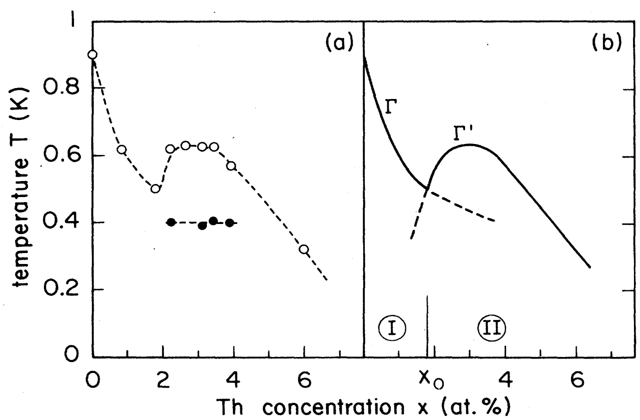

FIG. 1. (a) Experimental phase diagram. The phase diagram shows the behavior of T_c in dependence of the Th concentration x. The empty dots denote the onset of the superconductivity, the black dots the additional transition. All these transitions are second-order transitions. The data are from Ref. 4. (b) Ideal phase diagram. x_0 separates the region I and II. In region I, Γ is the dominant irreducible representation [$T_c(\Gamma,x)>T_c(\Gamma',x)$] and in region II Γ' is dominant [$T_c(\Gamma,x)<T_c(\Gamma',x)$].

The recent series of experiments on the influence of a uniform pressure on the transition temperature in $U_{1-x}Th_xBe_{13}$ for different values of x by Lambert *et al.* support this assumption.[15] They observed a strong suppression of T_c with pressure, but an important result was the very different values of the coefficient dT_c/dP in the two regions I and II.

If we write

$$\begin{aligned} T_c(\Gamma,x,P)&=T_c(\Gamma,x)-K(\Gamma)P\ ,\\ T_c(\Gamma',x,P)&=T_c(\Gamma',x)-K(\Gamma')P\ , \end{aligned} \tag{4}$$

then the experimental values of the coefficients are $K(\Gamma)\approx 0.022$ K/kbar and $K(\Gamma')\approx 0.07$ K/kbar. Note a linear dependence is in rather good agreement with experiment. Near x_0 we can expand $T_c(\Gamma(\Gamma'),x)$ with respect to x also,

$$\begin{aligned} T_c(\Gamma,x)&=T_c(\Gamma,\tilde{x}_0)+a(x-\tilde{x}_0)\ ,\\ T_c(\Gamma',x)&=T_c(\Gamma',\tilde{x}_0)+b(x-\tilde{x}_0)\ , \end{aligned} \tag{5}$$

with $\tilde{x}_0=x_0(P=0)$. The linear coefficients a and b are slightly pressure dependent; though we approximate them simply by the values at $P=2$ kbar: $a\approx -15$ K and $b\approx 13$ K. The critical $x_0(P)$ can be calculated now from the relation

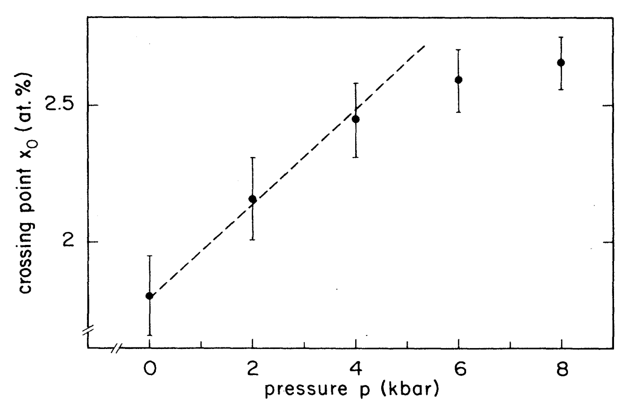

FIG. 2. The dependence of x_0 on an applied uniform pressure. The data of the black points are extracted from the experimental results of Ref. 15. The dashed line is the linear approach in Sec. II.

$$T_c(\Gamma,x_0(P),P)=T_c(\Gamma',x_0(P),P)\ ,$$

$$x_0(P)=\bar{x}_0+\frac{K(\Gamma)-K(\Gamma')}{a-b}P=0.018+0.0017P\ . \quad (6)$$

The form of the P dependence of x_0 is well described by this approach (Fig. 2). The deviation for large values P, however, is due to the pressure dependence of a and b which was disregarded. The model of a crossing of two different types of superconductivity at x_0 gives a consistent description of the (P,t) phase diagram.

III. THE GINZBURG-LANDAU EXPANSION NEAR x_0

For values of $x \approx x_0$, both representations Γ and Γ' become relevant since their T_c values are nearly equal. The Ginzburg-Landau (GL) expansion of the free energy, then, is composed of three parts: two separate parts F_Γ and $F_{\Gamma'}$ for the irreducible representations Γ and Γ', respectively, and the terms, which coupled the order parameters of these two representations,

$$F(\lambda)=F_\Gamma(\lambda(\Gamma,m))+F_{\Gamma'}(\lambda(\Gamma',m)) + F_{\Gamma,\Gamma'}(\lambda(\Gamma,m),\lambda(\Gamma',m))\ . \quad (7)$$

F_Γ and $F_{\Gamma'}$ are known from Sec. I. The coupling terms which connect the order parameters must be invariant under the operations of the point group O, the time reversal, and the U(1) gauge symmetry. No such invariant second-order terms can be constructed. The order of the first possible invariant terms is four. They can be easily formed by considering the fourfold Kronecker products of the representations.

$$\Gamma^*\otimes\Gamma\otimes\Gamma'^*\otimes\Gamma'\ , \quad (8a)$$

$$\Gamma^*\otimes\Gamma^*\otimes\Gamma'\otimes\Gamma'\ , \quad (8b)$$

$$\Gamma^*\otimes\Gamma'^*\otimes\Gamma'\otimes\Gamma'\ , \quad (8c)$$

$$\Gamma^*\otimes\Gamma^*\otimes\Gamma\otimes\Gamma'\ . \quad (8d)$$

The asterisk denotes the complex conjugation of the corresponding order-parameter basis. Note that we have to add the complex conjugate in Eqs. (8b)–(8d) in order to satisfy time reversal. In general, before adding the complex conjugate terms, we can multiply these terms by global phase factors $\exp(i\gamma)$. To fulfill the point group invariance, we decompose these products and keep only the Γ_1 components with its (Clebsch-Gordan) combined basis function, which are the only invariant combination terms of fourth order. Then we select the basis functions in order to obtain only linearly independent invariant terms (Table III). $F_{\Gamma,\Gamma'}$ is a linear combination of these terms with a set of undetermined coefficients θ_i.

The combinations in Eqs. (8a) and (8b) can cause new second-order transitions. The latter terms link the phase factors of the two-order parameter basis functions, as will be shown in the following sections. Eqs. (8c) and (8d) are linear in the order parameter of one representation, and cubic in the other one. They can cause first-order transitions and a "screening"or suppression of some second-order transitions expected from Eqs. (8a) and (8b). Because of the rather complicated structure of these coupling terms, and the many possibilities, we cannot discuss the general behavior of the GL expansion. Instead we will examine only some special cases to show how various types of phase diagrams can arise.

TABLE III. Invariant fourth-order terms, which couple the different representations. These combinations are obtained from the decomposition of the fourfold Kronecker products of the two involved representations (Γ,Γ') and the application of the Clebsch-Gordan formalism. The θ_i and γ_i are real numbers and not determined coefficients and phase factors, respectively, of these terms in the GL expansion.

(Γ,Γ')	Product	Invariant terms	Coefficient
(Γ_1,Γ_3)	$\Gamma_1^*\otimes\Gamma_1\otimes\Gamma_3^*\otimes\Gamma_3$	$\|\lambda_1\|^2(\|\lambda_2\|^2+\|\lambda_3\|^2)$	θ_1
	$\Gamma_1^*\otimes\Gamma_1^*\otimes\Gamma_3\otimes\Gamma_3$	$e^{i\gamma_2}\lambda_1^{*2}(\lambda_2^2+\lambda_3^2)+\text{c.c.}$	θ_2
	$\Gamma_1^*\otimes\Gamma_3\otimes\Gamma_3^*\otimes\Gamma_3$	$e^{i\gamma_3}\lambda_1^*(\lambda_2\|\lambda_2\|^2-2\lambda_2\|\lambda_3\|^2-\lambda_2^*\lambda_3^2)+\text{c.c.}$	θ_3
	$\Gamma_1^*\otimes\Gamma_1\otimes\Gamma_1^*\otimes\Gamma_3$	no Γ_1 component	
(Γ_1,Γ_4)	$\Gamma_1^*\otimes\Gamma_1\otimes\Gamma_4^*\otimes\Gamma_4$	$\|\lambda_1\|^2(\|\lambda_4\|^2+\|\lambda_5\|^2+\|\lambda_6\|^2)$	θ_1
	$\Gamma_1^*\otimes\Gamma_1^*\otimes\Gamma_4\otimes\Gamma_4$	$e^{i\gamma_2}\lambda_1^{*2}(\lambda_4^2+\lambda_5^2+\lambda_6^2)+\text{c.c.}$	θ_2
	$\Gamma_1^*\otimes\Gamma_4\otimes\Gamma_4^*\otimes\Gamma_4$	$e^{i\gamma_3}\lambda_1^*[\lambda_4(\lambda_5^*\lambda_6-\lambda_5\lambda_6^*)+\lambda_5(\lambda_6^*\lambda_4-\lambda_6\lambda_4^*)$ $+\lambda_6(\lambda_4^*\lambda_5-\lambda_4\lambda_5^*)]+\text{c.c.}$	θ_3
	$\Gamma_1^*\otimes\Gamma_1\otimes\Gamma_1^*\otimes\Gamma_4$	no Γ_1 component	
(Γ_1,Γ_5)	$\Gamma_1^*\otimes\Gamma_1\otimes\Gamma_5^*\otimes\Gamma_5$	$\|\lambda_1\|^2(\|\lambda_7\|^2+\|\lambda_8\|^2+\|\lambda_9\|^2)$	θ_1
	$\Gamma_1^*\otimes\Gamma_1^*\otimes\Gamma_5\otimes\Gamma_5$	$e^{i\gamma_2}\lambda_1^{*2}(\lambda_7^2+\lambda_8^2+\lambda_9^2)+\text{c.c.}$	θ_2
	$\Gamma_1^*\otimes\Gamma_5\otimes\Gamma_5^*\otimes\Gamma_5$	$e^{i\gamma_3}\lambda_1^*[\lambda_7(\lambda_8^*\lambda_9+\lambda_8\lambda_9^*)+\lambda_8(\lambda_9^*\lambda_7+\lambda_9\lambda_7^*)$ $+\lambda_9(\lambda_7^*\lambda_8+\lambda_7\lambda_8^*)]+\text{c.c.}$	θ_3
	$\Gamma_1^*\otimes\Gamma_1\otimes\Gamma_1^*\otimes\Gamma_5$	no Γ_1 component	

TABLE III. (*Continued*).

(Γ,Γ')	Product	Invariant terms	Coefficient
(Γ_3,Γ_4)	$\Gamma_3^*\otimes\Gamma_3\otimes\Gamma_4^*\otimes\Gamma_4$	$(\lvert\lambda_2\rvert^2+\lvert\lambda_3\rvert^2)(\lvert\lambda_4\rvert^2+\lvert\lambda_5\rvert^2+\lvert\lambda_6\rvert^2)$	θ_1
		$(\lvert\lambda_3\rvert^2-\lvert\lambda_2\rvert^2)(\lvert\lambda_4\rvert^2+\lvert\lambda_5\rvert^2-2\lvert\lambda_6\rvert^2)$ $+\sqrt{3}(\lambda_2^*\lambda_3+\lambda_2\lambda_3^*)(\lvert\lambda_5\rvert^2-\lvert\lambda_4\rvert^2)$	θ_2
	$\Gamma_3^*\otimes\Gamma_3^*\otimes\Gamma_4\otimes\Gamma_4$	$e^{i\gamma_3}(\lambda_2^{*2}+\lambda_3^{*2})(\lambda_4^2+\lambda_5^2+\lambda_6^2)+\text{c.c.}$	θ_3
		$e^{i\gamma_4}[(\lambda_3^{*2}-\lambda_2^{*2})(\lambda_4^2+\lambda_5^2-2\lambda_6^2)$ $+2\sqrt{3}\lambda_2^*\lambda_3^*(\lambda_5^2-\lambda_4^2)]+\text{c.c.}$	θ_4
	$\Gamma_3^*\otimes\Gamma_4\otimes\Gamma_4^*\otimes\Gamma_4$	$e^{i\gamma_5}[\lambda_2^*\{\lambda_4(\lambda_5^*\lambda_6-\lambda_5\lambda_6^*)+\lambda_5(\lambda_6^*\lambda_4-\lambda_6\lambda_4^*)$ $-2\lambda_6(\lambda_4^*\lambda_5-\lambda_4\lambda_5^*)\}+\sqrt{3}\lambda_3^*\{\lambda_5(\lambda_6^*\lambda_4-\lambda_6\lambda_4^*)$ $-\lambda_4(\lambda_5^*\lambda_6-\lambda_5\lambda_6^*)\}]+\text{c.c.}$	θ_5
		$e^{i\gamma_6}[\sqrt{3}\lambda_2^*\{\lambda_5(\lambda_6^*\lambda_4+\lambda_6\lambda_4^*)+\lambda_4(\lambda_5^*\lambda_6+\lambda_5\lambda_6^*)\}$ $+\lambda_3^*\{\lambda_4(\lambda_5^*\lambda_6+\lambda_5\lambda_6^*)+\lambda_5(\lambda_6^*\lambda_4+\lambda_6\lambda_4^*)$ $-2\lambda_6(\lambda_4^*\lambda_5+\lambda_4\lambda_5^*)\}]+\text{c.c.}$	θ_6
	$\Gamma_3^*\otimes\Gamma_3\otimes\Gamma_3^*\otimes\Gamma_4$	no Γ_1 component	
(Γ_3,Γ_5)	$\Gamma_3^*\otimes\Gamma_3\otimes\Gamma_5^*\otimes\Gamma_5$	$(\lvert\lambda_2\rvert^2+\lvert\lambda_3\rvert^2)(\lvert\lambda_7\rvert^2+\lvert\lambda_8\rvert^2+\lvert\lambda_9\rvert^2)$	θ_1
		$(\lvert\lambda_3\rvert^2-\lvert\lambda_2\rvert^2)(\lvert\lambda_7\rvert^2+\lvert\lambda_8\rvert^2-2\lvert\lambda_9\rvert^2)+\sqrt{3}(\lambda_2^*\lambda_3+\lambda_2\lambda_3^*)(\lvert\lambda_8\rvert^2-\lvert\lambda_7\rvert^2)$	θ_2
	$\Gamma_3^*\otimes\Gamma_3^*\otimes\Gamma_5\otimes\Gamma_5$	$e^{i\gamma_3}(\lambda_2^{*2}+\lambda_3^{*2})(\lambda_7^2+\lambda_8^2+\lambda_9^2)+\text{c.c.}$	θ_3
		$e^{i\gamma_4}[(\lambda_3^{*2}-\lambda_2^{*2})(\lambda_7^2+\lambda_8^2-2\lambda_9^2)+2\sqrt{3}\lambda_2^*\lambda_3^*(\lambda_8^{*2}-\lambda_7^{*2})]+\text{c.c.}$	θ_4
	$\Gamma_3^*\otimes\Gamma_5\otimes\Gamma_5^*\otimes\Gamma_5$	$e^{i\gamma_5}[\lambda_2^*\{\lambda_7(\lambda_8^*\lambda_9+\lambda_8\lambda_9^*)+\lambda_8(\lambda_9^*\lambda_7+\lambda_9\lambda_7^*)$ $-2\lambda_9(\lambda_7^*\lambda_8+\lambda_7\lambda_8^*)\}+\sqrt{3}\lambda_3^*\{\lambda_8(\lambda_9^*\lambda_7+\lambda_9\lambda_7^*)$ $-\lambda_7(\lambda_8^*\lambda_9+\lambda_8\lambda_9^*)\}]+\text{c.c.}$	θ_5
		$e^{i\gamma_6}[\sqrt{3}\lambda_2^*\{\lambda_7(\lambda_8^*\lambda_9+\lambda_8\lambda_9^*)-\lambda_8(\lambda_9^*\lambda_7+\lambda_9\lambda_7^*)\}$ $+\lambda_3^*\{\lambda_7(\lambda_8^*\lambda_9+\lambda_8\lambda_9^*)+\lambda_8(\lambda_9^*\lambda_7+\lambda_9\lambda_7^*)$ $-2\lambda_9(\lambda_7^*\lambda_8+\lambda_7\lambda_8^*)\}]+\text{c.c.}$	θ_6
	$\Gamma_3^*\otimes\Gamma_3\otimes\Gamma_3^*\otimes\Gamma_5$	no Γ_1 component	
(Γ_4,Γ_5)	$\Gamma_4^*\otimes\Gamma_4\otimes\Gamma_5^*\otimes\Gamma_5$	$(\lambda_4\rvert^2+\lvert\lambda_5\rvert^2+\lvert\lambda_6\rvert^2)(\lvert\lambda_7\rvert^2+\lvert\lambda_8\rvert^2+\lvert\lambda_9\rvert^2)$	θ_1
		$(\lvert\lambda_4\rvert^2+\lvert\lambda_5\rvert^2-2\lvert\lambda_6\rvert^2)(\lvert\lambda_7\rvert^2+\lvert\lambda_8\rvert^2-2\lvert\lambda_9\rvert^2)$ $+3(\lvert\lambda_4\rvert^2-\lvert\lambda_5\rvert^2)(\lvert\lambda_7\rvert^2-\lvert\lambda_8\rvert^2)$	θ_2
		$(\lambda_5^*\lambda_6-\lambda_5\lambda_6^*)(\lambda_8^*\lambda_9-\lambda_8\lambda_9^*)$ $+(\lambda_6^*\lambda_4-\lambda_6\lambda_4^*)(\lambda_9^*\lambda_7-\lambda_9\lambda_7^*)$ $+(\lambda_4^*\lambda_5-\lambda_4\lambda_5^*)(\lambda_7^*\lambda_8-\lambda_7\lambda_8^*)$	θ_3
		$(\lambda_5^*\lambda_6+\lambda_5\lambda_6^*)(\lambda_8^*\lambda_9+\lambda_8\lambda_9^*)$ $+(\lambda_6^*\lambda_4+\lambda_6\lambda_4^*)(\lambda_9^*\lambda_7+\lambda_9\lambda_7^*)$ $+(\lambda_4^*\lambda_5+\lambda_4\lambda_5^*)(\lambda_7^*\lambda_8+\lambda_7\lambda_8^*)$	θ_4
	$\Gamma_4^*\otimes\Gamma_4^*\otimes\Gamma_5\otimes\Gamma_5$	$e^{i\gamma_5}(\lambda_4^{*2}+\lambda_5^{*2}+\lambda_6^{*2})(\lambda_7^2+\lambda_8^2+\lambda_9^2)+\text{c.c.}$	θ_5
		$e^{i\gamma_6}[(\lambda_4^{*2}+\lambda_5^{*2}-2\lambda_6^{*2})(\lambda_7^2+\lambda_8^2-2\lambda_9^2)$ $+3(\lambda_4^{*2}-\lambda_5^{*2})(\lambda_7^2-\lambda_8^2)]+\text{c.c.}$	θ_6
		$e^{i\gamma_7}[\lambda_5^*\lambda_6^*\lambda_8\lambda_9+\lambda_4^*\lambda_6^*\lambda_7\lambda_9+\lambda_4^*\lambda_5^*\lambda_7\lambda_8]+\text{c.c.}$	θ_7
	$\Gamma_4^*\otimes\Gamma_5\otimes\Gamma_5^*\otimes\Gamma_5$	$e^{i\gamma_8}[\lambda_4^*\lambda_7(\lvert\lambda_8\rvert^2-\lvert\lambda_9\rvert^2)+\lambda_5^*\lambda_8(\lvert\lambda_9\rvert^2$ $-\lvert\lambda_7\rvert^2)+\lambda_6^*\lambda_9(\lvert\lambda_7\rvert^2-\lvert\lambda_8\rvert^2)]$ c.c.	θ_8
		$e^{i\gamma_9}[\lambda_4^*\lambda_7^*(\lambda_8^2-\lambda_9^2)+\lambda_5^*\lambda_8^*(\lambda_9^2-\lambda_7^2)$ $+\lambda_6^*\lambda_9^*(\lambda_7^2-\lambda_8^2)]+\text{c.c.}$	θ_9
	$\Gamma_5^*\otimes\Gamma_4\otimes\Gamma_4^*\otimes\Gamma_5$	$e^{i\gamma_{10}}[\lambda_7^*\lambda_4(\lvert\lambda_5\rvert^2-\lvert\lambda_6\rvert^2)+\lambda_8^*\lambda_5(\lvert\lambda_6\rvert^2$ $-\lvert\lambda_4\rvert^2)+\lambda_9^*\lambda_6(\lvert\lambda_4\rvert^2-\lvert\lambda_5\rvert^2)]+\text{c.c.}$	θ_{10}
		$e^{i\gamma_{11}}[\lambda_7^*\lambda_4^*(\lambda_5^2-\lambda_6^2)+\lambda_8^*\lambda_5^*(\lambda_6^2-\lambda_4^2)$ $+\lambda_9^*\lambda_6^*(\lambda_4^2-\lambda_5^2)]+\text{c.c.}$	θ_{11}

IV. THE COMBINATION OF Γ_1 and Γ_i

In the next three sections the question, whether it is possible to fit the phase diagram [Fig. 1(a)] with the proposed model will be examined. We will restrict ourselves to phase diagrams where (1) the state in region I has some point zeros in the gap in order to explain the T^3 law of the specific heat in UBe_{13} at low T; (2) at least one additional second-order transition must occur in region II below T_c, but none in region I for small values of $x(<0.015)$. There is a rich variety of additional transitions possible similar to the situation under uniaxial stress that we examined previously.[22]

A. Γ_1 and Γ_3

We begin by discussing one of the simplest examples, namely the crossing of the Γ_1 and Γ_3 representation. Even for this case a complete analytic solution is not possible—a fact which reflects the complexity that can occur in many component GL theories. Often only numerical investigations are tractable.

Specifically in this example, it is the term due to the combination $\Gamma_1 \otimes \Gamma_3 \otimes \Gamma_3 \otimes \Gamma_3$ which forms the main obstacle for a simple treatment.

$$\begin{aligned} f = {} & A_1(T)|\lambda_1|^2+\beta|\lambda_1|^4+A_3(T)(|\lambda_2|^2+|\lambda_3|^2)+\beta_1(|\lambda_2|^2+|\lambda_3|^2)^2 \\ & +\beta_2(\lambda_2^*\lambda_3-\lambda_2\lambda_3^*)^2+\theta_1|\lambda_1|^2(|\lambda_2|^2+|\lambda_3|^2)+\frac{\theta_2}{2}[e^{i\gamma_2}\lambda_1^{*2}(\lambda_2^2+\lambda_3^2)+\text{c.c.}] \\ & +\frac{\theta_3}{\sqrt{2}}[e^{i\gamma_3}\lambda_i^*(\lambda_2|\lambda_2|^2-2\lambda_2|\lambda_3|^2-\lambda_2^*\lambda_3^2)+\text{c.c.}] , \end{aligned} \tag{9}$$

with

$$A_i(T)=T/T_c(\Gamma_i/x)-1 .$$

In the future we shall use the short notation $T_i=T_c(\Gamma_i,x)$. A transformation in the Γ_3 vector space leads to a more convenient form of F, setting

$$\lambda_2=\frac{1}{\sqrt{2}}(\lambda_2'+\lambda_3'), \quad \lambda_3=\frac{i}{\sqrt{2}}(\lambda_2'-\lambda_3') ,$$

and writing

$$\lambda_1=|\lambda_1|e^{i\phi_i}, \quad \lambda_2'=|\lambda|e^{i\phi_2}\cos\psi, \quad \lambda_3'=|\lambda|e^{i\phi_3}\sin\psi .$$

This transformation is closely related to the gap function five of Blount's classification[8] $[\mathbf{d}(\mathbf{k})\sim\hat{\mathbf{x}}k_x+\epsilon\hat{\mathbf{y}}k_y+\epsilon^2\hat{\mathbf{z}}k_z, \epsilon=e^{i2\pi/3}]$. The new form of the free energy has the advantage that the explicit dependence on the phase factors is restricted to the θ_2 and θ_3 terms and is

$$f=A_1(T)|\lambda_1|^2+\beta|\lambda_1|^4+A_3(T)|\lambda|^2+Q_1|\lambda|^4+Q_2|\lambda_1|^2|\lambda|^2+Q_3|\lambda_1||\lambda|^3 , \tag{10}$$

where $Q_1=\beta_1-\beta_2\cos^2(2\psi)$, $Q_2=\theta_1+\theta_2\sin(2\psi)\cos(2\phi_1-\phi_2-\phi_3-\gamma_2)$, and $Q_3=\theta_3\sin(2\psi)\cos\psi\cos(\phi_1+\phi_3-2\phi_2-\gamma_3)+\sin\psi\cos(\phi_1+\phi_2-2\phi_3-\gamma_3)$.

The order parameter immediately below T_c should belong to a single representation (SR) and at lower temperatures may make a transition to a combined representation (CR) phase $\Gamma_1\oplus\Gamma_3$. Neglecting for the moment the θ_3 term, there are three possible SR states, according as $T_1 \lessgtr T_3$:

$$|\lambda_1|^2=-\frac{A_1}{2\beta}, |\lambda|=0 , \tag{11a}$$

$$|\lambda|^2=-\frac{A_3}{2Q_1}, |\lambda_1|=0, \psi=\begin{cases} \frac{\pi}{4} & \beta_2<0, \quad (11b) \\ 0, \frac{\pi}{2} & \beta_2>0. \quad (11c) \end{cases}$$

As mentioned in Refs. 6 and 7, the order parameter of Eq. (11b) is not fully determined by the fourth-order terms, so that sixth-order terms are required. However it is beyond our intention to extend the scope of this work to also examine sixth-order terms.

It is further possible to calculate the CR state from Eq. (10),

$$|\lambda_1|^2=\frac{A_3Q_2-A_1Q_1}{2\beta Q_1-Q_2^2}, \quad |\lambda|^2=\frac{A_1Q_2-2\beta A_3}{2\beta Q_1-Q_2^2} , \tag{12a}$$

with

$$T_1^{(0)}=T_3\frac{1-G}{1-G\dfrac{T_3}{T_1}}, \quad G=\frac{Q_2}{2\beta} . \tag{12b}$$

Note that this state is completely determined even for $\beta_2>0$. Considering now the special case $T_1>T_3$ and $\theta_2>0$ $(\gamma_i=0)$, we see at $T_1^{(0)}$ an additional second-order transition replacing the SR phase of Eq. (11a). The value of ψ is fixed at $\pi/4$ [as long as $|\lambda|^2<\theta_2|\lambda_1|^2/2\beta_2$, similar to the condition in Eq. (21)] and $\phi_2+\phi_3=\pi$ ($\phi_1=0$).

If we turn on the θ_3 term, this additional second-order transition can become unstable against a first-order transition to a CR phase, since this term introduces quasi-third-order combinations of $|\lambda|$ which lead to such instabilities. The angle ψ cannot be fixed in the CR phase, but deviates smoothly from $\pi/4$. Taking into account, however, that Q_3 is zero for the considered values $\psi=\pi/4$ and $\phi_2=\phi_3=0$, we show in the Appendix that the effective term in $|\lambda_1|$ and $|\lambda|$ related with Q_3 do not prevent the continuous transition at $T_1^{(0)}$. This holds true if the modulus of θ_3 is not much larger than θ_2, otherwise it would be more favorable to choose ϕ_2 and ϕ_3 so that Q_3 adopts the attainable most negative values in the CR phase (e.g., $\phi_2=\phi_3=\pi$). Therefore, in the case of "large" θ_3, the additional second-order transition is preempted by a first-order one (a jump from the SR phase with $\lambda=0$ to a CR phase with finite λ and the most negative value for Q_3). It is a question of a competition among the θ_2 and θ_3 terms, but it is very difficult to give a good threshold for the ratio θ_2/θ_3 (see Ref. 23).

Under the other assumption, $T_3>T_1$, a SR phase of Γ_3 is prevented in the case $\beta_2<0$, since we have a finite admixture of the Γ_1 component due to the linear dependence of the θ_3 term on $|\lambda_1|$ as proved in Ref. 10. In the case $\beta_2>0$, only a first-order transition can take place from the SR phase [Eq. (11c)] and the CR phase (see the Appendix).

Since the continuous attainable CR phase, including the θ_3 term ($\theta_3<\theta_2$), has a rather more complicated form than in Eq. (12), and because of a group-theoretical reason which becomes obvious in Sec. VIII, we prefer not to discuss this example further in connection with the additional phase transition. For this purpose the next example is more suitable.

B. Γ_1 and Γ_4 or Γ_5

Both combinations (Γ_1,Γ_4) and (Γ_1,Γ_5) are very similar. For a reason which will become clear later in Sec. 8, we concentrate on the choice (Γ_1,Γ_5). Writing again, $\lambda_j=|\lambda_j|e^{i\phi_j}$, the GL expansion takes the form in this case

$$\begin{aligned}
f=&A_1(T)|\lambda_1|^2+\beta|\lambda_1|^4+A_5(T)(|\lambda_7|^2+|\lambda_8|^2+|\lambda_9|^2)+\eta_1'(|\lambda_7|^2+|\lambda_8|^2+|\lambda_9|^2)^2\\
&+\eta_2'[|\lambda_7|^4+|\lambda_8|^4+|\lambda_9|^4+2|\lambda_7|^2|\lambda_8|^2\cos(2\phi_7-2\phi_8)\\
&\quad+2|\lambda_7|^2|\lambda_9|^2\cos(2\phi_7-2\phi_9)+2|\lambda_8|^2|\lambda_9|^2\cos(2\phi_8-2\phi_9)]\\
&+\eta_3'(|\lambda_7|^2|\lambda_8|^2+|\lambda_7|^2|\lambda_9|^2+|\lambda_8|^2|\lambda_9|^2)+\theta_1|\lambda_1|^2(|\lambda_7|^2+|\lambda_8|^2+|\lambda_9|^2)\\
&+\theta_2|\lambda_1|^2[|\lambda_y|^2\cos(2\phi_7-2\phi_1+\gamma_2)+|\lambda_8|^2\cos(2\phi_8-2\phi_1+\gamma_2)+|\lambda_9|^2\cos(2\phi_9-2\phi_1+\gamma_2)]\\
&+\theta_3|\lambda_1||\lambda_7||\lambda_8||\lambda_9|[\cos(\phi_9-\phi_8)\cos(\phi_7-\phi_1)\\
&\qquad+\cos(\phi_7-\phi_9)\cos(\phi_8-\phi_1)+\cos(\phi_8-\phi_7)\cos(\phi_9-\phi_1)]\ .
\end{aligned}\tag{13}$$

There are very many possibilities now. We restrict our attention to the most interesting case $0<4\eta_2'<\eta_3'$. Then the SR order parameter of Γ_5 consists of only one component (λ_7, λ_8, λ_9), e.g.,

$$|\lambda_7|^2=-\frac{A_5}{2(\eta_1'+\eta_2')},\quad \lambda_1=\lambda_8=\lambda_9=0\ . \tag{14}$$

The SR order parameter of Γ_1 has the form quoted already in Eq. (12a). Second-order transitions between a CR order parameter ($\Gamma_1\oplus\Gamma_5$) and both SR phases are allowed. The CR phase has the order parameter

$$|\lambda_7|^2=\frac{A_1Q-2\beta A_5}{4\beta(\eta_1'+\eta_2')-Q^2},\quad |\lambda_1|^2=\frac{A_5Q-2(\eta_1'+\eta_2')A_1}{4\beta(\eta_1'+\eta_2')-Q^2}\ ,$$

$$\lambda_8=\lambda_9=0,\phi_7-\phi_1=\begin{cases}-\dfrac{\gamma_2}{2},\pi-\dfrac{\gamma_2}{2}, & \theta_2<0,\\[2ex] \dfrac{\pi-\gamma_2}{2},\dfrac{3\pi-\gamma_2}{2}, & \theta_2>0,\end{cases} \tag{15}$$

and the transitions $\Gamma_5\to\Gamma_1\oplus\Gamma_5$ and $\Gamma_1\to\Gamma_1\oplus\Gamma_5$ occur at temperatures

$$T_5^{(0)}=T_1\frac{1-G}{1-G\dfrac{T_1}{T_5}},\quad G=\frac{Q}{2(\eta_1'+\eta_2')}\ , \tag{16a}$$

$$T_1^{(0)}=T_5\frac{1-G'}{1-G'\dfrac{T_5}{T_1}},\quad G'=\frac{Q}{2\beta}\ , \tag{16b}$$

respectively, where $Q=\theta_1-|\theta_2|$. For the existence of the CR state it is necessary that

$$4\beta(\eta_1'+\eta_2')-Q^2>0\ ,$$

and, additionally, it is required that for $(T_1>T_5)$ $Q<2\beta$, and for $(T_1<T_5)Q<2(\eta_1'+\eta_2')$. Note that these second-order transitions are not affected by the θ_3 term, which

TABLE IV. CR states of the combination (Γ_1,Γ_5). These even- and odd-parity states are nonunitary and 12-fold degenerate. The symmetry is orthorhombic.

θ_2	Odd-parity states $\mathbf{d}(\mathbf{k})$	Even parity states $\psi(\mathbf{k})$
$\theta_2<0$	$\frac{\lvert\lambda_1\rvert}{\sqrt{3}}(\hat{\mathbf{x}}k_x+\hat{\mathbf{y}}k_y+\hat{\mathbf{z}}k_z)\pm\frac{\lvert\lambda_j\rvert}{\sqrt{2}}\times\begin{Bmatrix}e^{i\gamma_2}\\ e^{-i\gamma_2}\end{Bmatrix}\times\begin{Bmatrix}\hat{\mathbf{y}}k_z+\hat{\mathbf{z}}k_y\\ \hat{\mathbf{z}}k_x+\hat{\mathbf{x}}k_z\\ \hat{\mathbf{x}}k_y+\hat{\mathbf{y}}k_x\end{Bmatrix}$	$\frac{\lvert\lambda_1\rvert}{\sqrt{3}}(k_x^2+k_y^2+k_z^2)\pm\sqrt{2}\lvert\lambda_j\rvert\begin{Bmatrix}e^{i\gamma_2}\\ e^{-i\gamma_2}\end{Bmatrix}\begin{Bmatrix}k_yk_z\\ k_zk_x\\ k_xk_y\end{Bmatrix}$
$\theta_2>0$	$\frac{\lvert\lambda_1\rvert}{\sqrt{3}}(\hat{\mathbf{x}}k_x+\hat{\mathbf{y}}k_y+\hat{\mathbf{z}}k_z)\pm i\frac{\lvert\lambda_j\rvert}{\sqrt{2}}\times\begin{Bmatrix}e^{i\gamma_z}\\ e^{-i\gamma_2}\end{Bmatrix}\times\begin{Bmatrix}\hat{\mathbf{y}}k_z+\hat{\mathbf{z}}k_y\\ \hat{\mathbf{z}}k_x+\hat{\mathbf{x}}k_z\\ \hat{\mathbf{x}}k_y+\hat{\mathbf{y}}k_x\end{Bmatrix}$	$\frac{\lvert\lambda_1\rvert}{\sqrt{3}}(k_x^2+k_y^2+k_z^2)\pm i\sqrt{2}\lvert\lambda_j\rvert\begin{Bmatrix}e^{i\gamma_2}\\ e^{-i\gamma_2}\end{Bmatrix}\begin{Bmatrix}k_yk_z\\ k_zk_x\\ k_xk_y\end{Bmatrix}$

vanish at all temperatures for this parameter choice. Therefore , in this case, a series of three consecutive second-order transitions can take place (e.g., $T_1<T_5$, normal$\to$SR$(\Gamma_1)\to$CR$(\Gamma_1\oplus\Gamma_5)\to$SR$(\Gamma_5)$, where the third transition only occurs if $Q>2(\eta_1'+\eta_2')$ without violating the condition for the existence of the CR phase). Note the symmetry of the $\Gamma_1\oplus\Gamma_5$ phase is orthorhombic and $\mathbf{d}(\mathbf{k})$ is nonunitary in this phase (Table IV).

Outside the range $(0<4\eta_2'<\eta_3')$ the analysis of F is much more complicated. Of course there can be additional second-order transitions in the superconducting phase, but there are also instabilities yielding first-order transitions which are rather difficult to treat analytically and even numerically. We shall not pursue this region in accordance with the philosophy of this work, which is to restrict our attention to the simplest cases with phase diagrams possibly relevant to experiment.

V. COMBINATIONS OF TWO HIGHER DIMENSIONAL REPRESENTATIONS

A. Γ_3 and Γ_4 or Γ_5

The behavior of the combinations (Γ_3,Γ_4) and (Γ_3,Γ_5) is very similar. So we consider only the former and again only certain cases. If we use the same transformation for Γ_3 as above $(\lambda_j=|\lambda_j|e^{i\phi_j})$, the GL free energy has the form

$$
\begin{aligned}
f=f_{\Gamma_3}+f_{\Gamma_4}&+\theta_1|\lambda|^2(|\lambda_4|^2+|\lambda_5|^2+|\lambda_6|^2)+\theta_2|\lambda|^2\sin(2\psi)[(|\lambda_4|^2+|\lambda_5|^2-2|\lambda_6|^2)\cos\Delta\phi+\sqrt{3}(|\lambda_5|^2-|\lambda_4|^2)\sin\Delta\phi]\\
&+\theta_3|\lambda|^2\sin(2\psi)[|\lambda_4|^2\cos(2\phi_4-\phi_2-\phi_3)+|\lambda_5|^2\cos(2\phi_5-\phi_2-\phi_3)+|\lambda_6|^2\cos(2\phi_6-\phi_2-\phi_3)]\\
&+\theta_4|\lambda|^2\{\cos^2\psi[2|\lambda_6|^2\cos(2\phi_2-2\phi_6)-|\lambda_4|^2\cos(2\phi_2-2\phi_4)-|\lambda_5|^2\cos(2\phi_2-2\phi_5)]\\
&\qquad+\sin^2\psi[2|\lambda_6|^2\cos(2\phi_3-2\phi_6)-|\lambda_4|^2\cos(2\phi_3-2\phi_4)-|\lambda_5|^2\cos(2\phi_3-2\phi_5)]\\
&\qquad+\sqrt{3}\sin^2\psi[|\lambda_4|^2\sin(2\phi_4-2\phi_3)-|\lambda_5|^2\sin(2\phi_5-2\phi_3)]\\
&\qquad-\sqrt{3}\cos^2\psi[|\lambda_4|^2\sin(2\phi_4-2\phi_2)-|\lambda_5|^2\sin(2\phi_5-2\phi_2)]\}\ ,
\end{aligned}
\tag{17}
$$

with $\Delta\phi=\phi_2-\phi_3$. In addition, there are $\Gamma_3\otimes\Gamma_4\otimes\Gamma_4\otimes\Gamma_4$ terms which have properties similar to the θ_3 term in Sec. IV B. For simplicity we have set $\gamma_3=\gamma_4=0$. Similarly, to the previous section there are second-order transitions between the SR and the CR phases in the case $0<4\eta_2<\eta_3$ and again the other regions of the η_2-η_3-parameter plane lead to Γ_4 states which cannot be simply analyzed. So we concentrate on this case and also take $\beta_2>0$ in the Γ_3 part of f to avoid the sixth-order terms.

The SR order parameters for both representations have the similar forms as in Sec. IV. The CR phase can be calculated simply under the condition that θ_2,θ_3, and θ_4 have values so that it is possible to miminize the corresponding parts of the free energy separately with respect to the phase factors. Thus, let us assume that θ_2,θ_3, and θ_4 are all positive. This is only one of many possible ways to satisfy this condition. The phase difference $\Delta\phi=\phi_2-\phi_3$ is determined now only by the θ_2 term, leading to the condition

$$
\begin{aligned}
(|\lambda_4|^2+|\lambda_5|^2-2|\lambda_6|^2)\sin(\Delta\phi)&\\
=\sqrt{3}(|\lambda_5|^2-|\lambda_4|^2)\cos(\Delta\phi)\ .&
\end{aligned}
\tag{18}
$$

In this case

$$|\lambda_4|\neq0,\quad |\lambda_5|=|\lambda_6|=0\ ,$$

this leads to $\Delta\phi=2\pi/3$. The relative phase between the

Γ_3 and Γ_4 order parameters is determined by the θ_3 and θ_4 terms.

$$\phi_4=\frac{1}{2}\left[-\frac{\pi}{3}+n\pi\right],\quad n \text{ an even integer }, \tag{19}$$

where we fix the overall U(1) gauge by setting $\phi_3=0$. This result leads to a rather simple determination of the angle ψ. The θ_4 term does not contribute and ψ obeys the simple equation

$$[2\beta_2|\lambda|^2\sin(2\psi)-(2\theta_2+\theta_3)|\lambda_4|^2]|\lambda|^2\cos(2\psi)=0\ . \tag{20}$$

For $|\lambda|\neq 0$ and $|\lambda_4|\neq 0$, there are two solutions possible,

$$\cos(2\psi)=0\ ,$$

or

$$\sin(2\psi)=\frac{(2\theta_2+\theta_3)|\lambda_4|^2}{2\beta_2|\lambda|^2}\ . \tag{21}$$

The second equation is only defined if the rhs is smaller than 1. Minimizing with respect to $|\lambda_i|$ we obtain

$$|\lambda|^2=\frac{Q_1A_4-2Q_3A_3}{4Q_2Q_3-Q_1^2}\ ,\qquad |\lambda_4|^2=\frac{Q_1A_3-2Q_2A_4}{4Q_2Q_3-Q_1^2}\ , \tag{22}$$

with

$$Q_1=\theta_1-(2\theta_2+\theta_3)\sin(2\psi)-2\theta_4\ ,$$

$$Q_2=\beta_1-\beta_2\cos^2(2\psi)\ ,$$

and

$$Q_3=\eta_1+\eta_2\ .$$

Let us assume that $T_4>T_3$, then we can list the possible transitions and the symmetry and degeneracy of the phases: (1) a second second-order transition to the SR phase of Γ_4 (tetragonal, threefold degenerate), (2) a second second-order transition ($T^{(1)}$) leads to the CR phase with $\psi=\pi/4$ and a relative phase of Eq. (19) (orthorhombic, 12-fold degenerate), (3) a third second-order transition ($T^{(2)}$) appears when the second Eq. (21) is obeyed, and in this case ψ varies with decreasing T (orthorhombic, 24-fold degenerate), and (4) a fourth second-order transition ($T^{(3)}$) leads to a SR phase of Γ_3 with $\psi=0$ or $\pi/2$ (cubic, two-fold degenerate); this last transition only takes place if $2Q_2<Q_1$, otherwise no energy is gained by such a transition.

The corresponding transition temperatures are given in the expression

$$T^{(i)}=T_4\frac{1-G^{(i)}}{1-G^{(i)}\dfrac{T_4}{T_3}}\ , \tag{23}$$

where

$$G^{(1)}=\frac{2Q_3}{Q_1}=\frac{2(\eta_1+\eta_2)}{\theta_1-2\theta_2+\theta_3-2\theta_4}\ ,$$

$$G^{(2)}=\frac{\dfrac{Q_1(2\theta_2+\theta_3)}{2\beta_2}+2Q_3}{Q_1+\dfrac{Q_2(2\theta_2+\theta_3)}{\beta_2}}\ ,$$

$$G^{(4)}=\frac{Q_1}{2Q_2}=\frac{\theta_1-2\theta_4}{\beta_1-\beta_2}\ .$$

In the next section we will see that the phase diagram with this choice is an attractive possibility to explain the experiments. We catalogue the pairing states in the CR state with the fixed ψ (i.e., $T^{(1)}<T<T^{(2)}$ or $T^{(2)}<T<T^{(1)}$) in Table V.

B. Γ_4 and Γ_5

Again we concentrate on the parameter choice $0<4\eta_2<\eta_3$ and $0<4\eta_2'<\eta_3'$. In this case the combination (Γ_4,Γ_5) has similar properties to those discussed earlier for (Γ_1,Γ_5). The SR phases take the form of Eq. (14), and there is a single CR phase with

$$|\lambda_4|^2=\frac{QA_5-2(\eta_1'+\eta_2')A_4}{4(\eta_1+\eta_2)(\eta_1'+\eta_2')-Q^2}\ ,$$

$$|\lambda_7|^2=\frac{QA_4-2(\eta_1+\eta_2)A_5}{4(\eta_1+\eta_2)(\eta_1'+\eta_2')-Q^2}\ ,$$

$$\phi_4-\phi_7=\begin{cases}\gamma,\gamma+\pi, & \theta_5+4\theta_6<0\ ,\\ \gamma+\dfrac{\pi}{2},\gamma+\dfrac{3\pi}{2}, & \theta_5+4\theta_6>0\ ,\end{cases} \tag{24}$$

$$\lambda_5=\lambda_6=\lambda_8=\lambda_9=0\ ,$$

where

$$Q=\theta_1+4\theta_2-2|\theta_5+4\theta_6|\ .$$

The symmetry of this phase is orthorhombic and it is 12-fold degenerate (Table VI). All properties of the transitions are the same as the case (Γ_1,Γ_5) and the formula for the transition temperature are easily adapted from that case.

TABLE V. CR states of the combination (Γ_3,Γ_4) These odd-parity states are nonunitary and 12-fold degenerate. The symmetry is orthorhombic.

$\frac{\lvert\lambda\rvert}{\sqrt{2}}(\hat{\mathbf{y}}k_y-\hat{\mathbf{z}}k_z)\pm\frac{\lvert\lambda_4\rvert}{\sqrt{2}}\times\begin{Bmatrix}e^{i\gamma}\\ e^{-i\gamma}\end{Bmatrix}\times(\hat{\mathbf{y}}k_z-\hat{\mathbf{z}}k_y)$
$\frac{\lvert\lambda\rvert}{\sqrt{2}}(\hat{\mathbf{z}}k_z-\hat{\mathbf{x}}k_x)\pm\frac{\lvert\lambda_5\rvert}{\sqrt{2}}\times\begin{Bmatrix}e^{i\gamma}\\ e^{-i\gamma}\end{Bmatrix}\times(\hat{\mathbf{z}}k_x-\hat{\mathbf{x}}k_z)$
$\frac{\lvert\lambda\rvert}{\sqrt{2}}(\hat{\mathbf{x}}k_x-\hat{\mathbf{y}}k_y)\pm\frac{\lvert\lambda_6\rvert}{\sqrt{2}}\times\begin{Bmatrix}e^{i\gamma}\\ e^{-i\gamma}\end{Bmatrix}\times(\hat{\mathbf{x}}k_y-\hat{\mathbf{y}}k_x)$

TABLE VI. CR states of the combination (Γ_4,Γ_5). These odd-parity states are nonunitary and 12-fold degenerate. The symmetry is orthorhombic.

$\frac{|\lambda_4|}{\sqrt{2}}(\hat{\mathbf{y}}k_z-\hat{\mathbf{z}}k_y)\pm\frac{|\lambda_7|}{\sqrt{2}}\times\begin{Bmatrix}e^{i\gamma}\\e^{-i\gamma}\end{Bmatrix}\times(\hat{\mathbf{y}}k_z+\hat{\mathbf{z}}k_y)$
$\frac{|\lambda_5|}{\sqrt{2}}(\hat{\mathbf{z}}k_x-\hat{\mathbf{x}}k_z)\pm\frac{|\lambda_8|}{\sqrt{2}}\times\begin{Bmatrix}e^{i\gamma}\\e^{-i\gamma}\end{Bmatrix}\times(\hat{\mathbf{z}}k_x+\hat{\mathbf{x}}k_z)$
$\frac{|\lambda_6|}{\sqrt{2}}(\hat{\mathbf{x}}k_y-\hat{\mathbf{y}}k_x)\pm\frac{|\lambda_9|}{\sqrt{2}}\times\begin{Bmatrix}e^{i\gamma}\\e^{-i\gamma}\end{Bmatrix}\times(\hat{\mathbf{x}}k_y+\hat{\mathbf{y}}k_x)$

VI. PHASE DIAGRAMS

In the last two sections we showed that under certain conditions it is possible to obtain additional second-order transitions below the onset of the superconductivity by considering the behavior of the order parameter in the combined GL expansion. We wish now to investigate if it is possible to fit the experimental phase diagram of $U_{1-x}Th_xBe_{13}$ with these models. Our description will be qualitative, if only because we have to extend the region of validity of GL theory and extrapolate the results in order to compare with experiment.

As a first example, we consider the case (Γ_1,Γ_5). In the identification of the SR phases in regions I ($x<x_0$) and II ($x>x_0$), we must keep in mind that we need an SR state with point zeros in the gap for UBe_{13}. Therefore, in region I, Γ_5 should be dominant with a SR state, e.g., $\mathbf{d}(\mathbf{k})\sim\hat{\mathbf{y}}k_z+\hat{\mathbf{z}}k_y$. Our next question regards, which phase is reached at the crossing point ($x=x_0$) immediately below T_c. We assume that the condition for the existence of the CR phase is satisfied at least in region II (i.e., $4\beta(\eta_1'+\eta_2')-Q^2>0$, and $2(\eta_1'+\eta_2')>Q$, since $T_1>T_5$). In this case a second-order transition $[T_1^{(0)}]$ takes place between the SR phase of Γ_1 and the CR phase of $\Gamma_1\oplus\Gamma_5$. Two different phase diagrams are possible then, distinguished by the condition $2\beta>Q$ and $2\beta<Q$. In the former case, the transition $[T_5^{(0)}]$ between the Γ_5 and $\Gamma_1\oplus\Gamma_5$ phase occurs in region I and the phase diagram has the form pictures in Fig. 3(a). Since for $x\approx x_0$ it would appear that the T_1 line has a rather large slope, the $T_5^{(0)}$ line would be even steeper, and so would not enter far into region I. In the latter case this transition happens as a third second-order transition in region II [Fig. 3(b)].

From the discussion of the specific-heat measurement, we will see that Q (i.e., the parameters θ_i) is x dependent (Q decreases with increasing x), whereas the other parameters β, η_1', and η_2' are roughly independent of x with the relation $0<\beta<\eta_1'+\eta_2'$ (indeed this relation excludes the case $2\beta<Q$). Therefore, the $T_1^{(0)}$ line decreases rather strongly for $x>x_0$, but soon becomes flatter because of the flattening of $T_5(x)$ and the further decrease of $Q(x)$. The qualitative form of thee phase diagrams is clearly a possible representation of the experiments.

Entirely equivalent phase diagrams are found also in the combinations (Γ_1,Γ_4) and (Γ_4,Γ_5), so that it is not possible to distinguish, on these grounds, between these possibilities. We can, however, say that the phase diagram in Fig. 3(a) looks the most relevant experimentally because of the relation $(\beta<\eta_1'+\eta_2')$.

Also, a similar behavior is expected for the combination of the representations Γ_3 and $\Gamma_4(\Gamma_5)$. In Sec. IV A a particular case was presented where we have shown that three second-order transitions, in addition to the normal-superconductor transition, can take place. Here we want to only consider the case that seems most relevant experimentally, $Q<2(\beta_1-\beta_2)$ and $Q<2(\eta_1+\eta_2)$, where we assume that the phase in region I in Γ_3 phase with $\beta_2>0$. In this case, a CR state minimizes the free energy, when $x=x_0$. Its form depends on the value of $G^{(2)}$ in Eq. (23), e.g., if $(0<G^{(3)}<G^{(2)}<1)$ then ψ (the relative phase of this state) is fixed, but if ψ $(1<G^{(2)}<G^{(1)})$ then ψ is temperature dependent. In the former case there are two second-order transitions rather

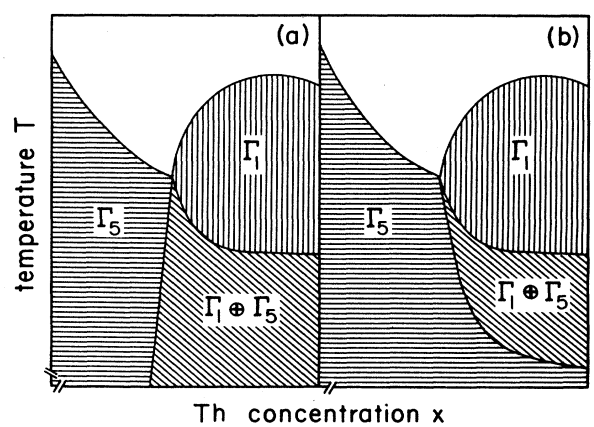

FIG. 3. Phase diagrams for (Γ_1,Γ_5). We consider only the two cases at the crossing point x_0: (a) $2(\eta_1'+\eta_2')>2\beta>Q$, $4\beta(\eta_1'+\eta_2')>Q^2$ ($T_5^{(0)}$ line in region I). (b) $2(\eta_1'+\eta_2')>Q>2\beta$, $4\beta(\eta_1'+\eta_2')>Q^2$ ($T_5^{(0)}$ line in region II). Q is assumed to decrease with enlarging x.

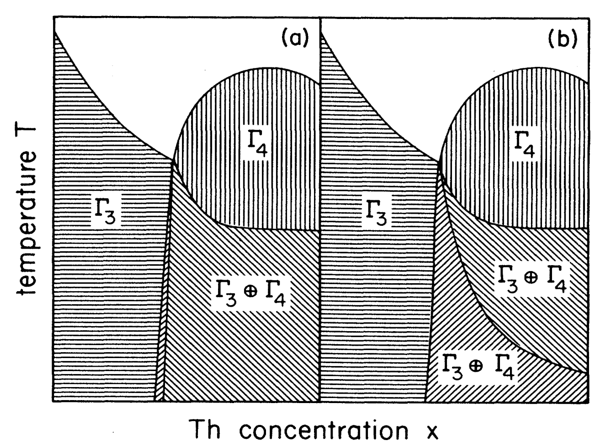

FIG. 4. Phase diagram for (Γ_3,Γ_5). Two different cases are considered: (a) $0<G^{(3)}<G^{(2)}<1$. (b) $1<G^{(2)}<G^{(1)}$. $G^{(i)}$ is defined in Eq. (23).

$(1 < G^{(2)} < G^{(1)})$ then ψ is temperature dependent. In the former case there are two second-order transitions rather close to each other in region I ($T^{(3)}$ and $T^{(2)}$) and only a single one in region II [Fig. 4(a)]. In the latter case the $T^{(2)}$ line lies in region II rather than in region I [Fig. 4(b)].

VII. SPECIFIC HEAT

We begin our discussion of the experimental data with the measurements of the specific heat of $U_{1-x}Th_xBe_{13}$. In the region II these show very clearly two separated discontinutiies marking the two second-order transitions. Although the description of our phenomenological calculations is only qualitative at the second transition for a sample with $x \approx 0.033$ in region II, we will still compare the experimental data with our results in order to estimate some of the parameters in the theory. The specific-heat C is given by the second derivative of F with respect to the temperature

$$C = -T\frac{\partial^2 F}{\partial T^2} , \tag{25}$$

so that we can calculate the discontinuties of C at the transition points for the example (Γ_1, Γ_5) using Eqs. (12) and (15) at the various transitions.

$$\Delta C_0 = \frac{\alpha}{2(\eta_1' + \eta_2')T_5} \quad (N \to \Gamma_5, T = T_5) , \tag{26a}$$

$$\Delta C_1 = \frac{\alpha}{2\beta T_1} \quad (N \to \Gamma_1, T = T_1) , \tag{26b}$$

$$\Delta C_2 = \frac{\alpha T_1^{(0)}}{T_1^2} \left[\frac{2Qr - 2\beta r^2 - 2(\eta_1' + \eta_2')}{Q^2 - 4\beta(\eta_1' + \eta_2')} - \frac{1}{2\beta} \right]$$
$$(\Gamma_1 \to \Gamma_1 \oplus \Gamma_5, T = T_1^{(0)}) . \tag{26c}$$

Note the ratio T_1/T_5, denoted by r, is not observable experimentally. The value of α is estimate to be

$$\alpha \approx 0.8 \times 10^{-27} T_c^2 J\ \mathrm{K}^{-2}\,\mathrm{mol}^{-1}$$

considering the free energy F per mol. The specific-heat discontinuity at $(N \to S)$ transition generally scales with the normal-state specific heat, i.e., the ratio $\Delta C/T_c$ should be independent of T_c which is rather well confirmed by the measurement of $\Delta C_0/T_5$ and $\Delta C_1/T_1$ in region I and II, respectively. The values of the ratios, however, show a clear difference between the two regions (see Table VII). This supports further the proposition that there are two different types of superconductivity in the two regions. From the knowledge of the magnitude of the discontinuities of the specific heat, we can estimate $2(\eta_1' + \eta_2')$, 2β, Q, and r. Using data from the Refs. 4 and 12, we give the results in Table VII for $x = 0$, 0.017, and 0.033. We have only one x in the region II because other values of x do not show well distinguished discontinuities in the specific heat. We obtain for $T_5(x = 0.033) \approx 0.43$ K, in agreement with a smooth extrapolation of the T_5 line drawn in Fig. 5. In order to fit the transition temperature for the second transition, it is necessary to assume a strong concentration dependence of the Q parameter, thus, at $x \approx 0.033$, $Q \approx 7 \times 10^{-29}$, but at $x \approx 0.022$, $Q \approx 2 \times 10^{-28}$. A linear extrapolation leads to a value at $x \approx x_0$ $Q(x_0 \approx 0.018) \approx 2.5 \times 10^{-28} < 2\beta$, which still satisfies the condition for the simple phase diagram in Fig. 3(a) of Sec. VI.

In summary, a consistent parametrization of the specific-heat data can be obtained within the framework of the simple phase diagram in Fig. 3(a).

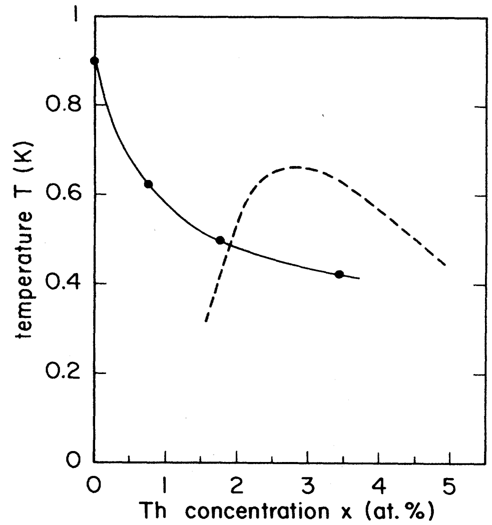

FIG. 5. The x dependence of $T_c(\Gamma_5, x)$. The values of $T_c(\Gamma_5, x)$ derived in Sec. VIII and catalogued in Table VII are plotted. The dashed line shows the x dependence of $T_c(\Gamma_1, x)$.

TABLE VII. Experimental data of the specific-heat measurements (Refs. 4 and 12). For three x values the onset of the supconductivity T_c with the corresponding discontinuity in specific heat $\Delta C_{0,1}/T_c$ (0 for region I, 1 for region II) and the additional transition point $T^{(0)}$ with $\Delta C_2/T^{(0)}$ for $x = 0.033$ are measured. Simple algebraic calculation leads to the values $T_c(\Gamma_5, x)$, 2β, and $2(\eta_1' + \eta_2')$ for the combination (Γ_1, Γ_5) (see also Fig. 5).

x (%)	T_c (K)	$T^{(0)}$ (K)	$\frac{\Delta C_{0,1}}{T_c}$ $\left[\frac{\mathrm{J}}{\mathrm{mol\,K}}\right]$	$\frac{\Delta C_2}{T^{(0)}}$ $\left[\frac{\mathrm{J}}{\mathrm{mol\,K}}\right]$	$T_c(\Gamma_5, x)$ (K)	$2(\eta_1' + \eta_2')$	2β
0	0.9		1.56		0.9	5.1×10^{-28}	
1.7	0.5		1.56		0.5	5.1×10^{-28}	
3.3	0.62	0.4	1.9	1.1	0.43		4.2×10^{-28}

VIII. ULTRASOUND ATTENUATION

Ultrasound measurements on the $U_{1-x}Th_xBe_{13}$ compound in region II show a sharp, rather large absorption peak at the second transition.[13,14] Joynt *et al.* tried to explain this fact by a dissipative domain-wall motion.[18] Because they used only superconducting states belonging to a single irreducible representation in the region II, their superconducting state had quite high symmetry (tetragonal or rhombohedral) so that no damping for a longitudinal sound wave in [111] direction was predicted from this mechanism. Such a damping, however, was observed in later experiments by Bishop *et al.*[14]

Superconducting CR states have lower symmetry so that damping is possible through this domain-wall mechanism. The sound wave couples to a domain wall if it induces a finite difference in the free energy between two domains (1 and 2) separated by the wall. In a simple model (viscous damping),[18] the sound attenuation is then proportional to the square of the free energy difference $(F_1-F_2)^2$. Assuming that the sound wavelength is much larger than the average extension of the domains, we calculate the change of the free energy via the coupling of a homogeneous strain ϵ to the order parameters

$$F_{\epsilon,\lambda}=\sum_{\gamma,m} C_1(\gamma)\epsilon(\gamma,m)V_1(\lambda,\gamma)_m + \sum_{\gamma',m'} C_5(\gamma')\epsilon(\gamma',m')V_5(\lambda,\gamma')_{m'} + \sum_{\gamma'',m''} C_{15}(\gamma'')\epsilon(\gamma'',m'')V_{15}(\lambda,\gamma'')_{m''} , \quad (27)$$

$\epsilon(\gamma,m)$ are the strain parameters (Table VIII), $V_i(\lambda,\gamma)_m$ are real bilinear forms of the order parameters (Table IX). They are built by the decomposition of the Kronecker products $\Gamma_1\otimes\Gamma_1$, $\Gamma_5\otimes\Gamma_5$, and $\Gamma_1\otimes\Gamma_5$, where γ, γ', and γ'' are its components (irreducible representations) and m, m', and m'' denotes their basis. $C_i(\gamma)$ are real coefficients. $F_{e,\lambda}$ contains all allowed coupling terms between the strain ϵ and the order parameters of Γ_1 and Γ_5.

A longitudinal sound wave in the [001] direction is characterized by $\epsilon_{zz}\neq 0$, $\epsilon_{xx}=\epsilon_{yy}=\epsilon_{ij}=0$ $(i\neq j)$, and in the [111] direction by $\epsilon_{xx}=\epsilon_{yy}=\epsilon_{zz}\neq 0$, $\epsilon_{xy}=\epsilon_{xz}=\epsilon_{yz}\neq 0$. For the [001] sound wave we consider the two domains of the CR phase corresonding to choices in 1 (2) of

TABLE VIII. Lattice strain parameters $\epsilon(\gamma,m)$ in a cubic system. The represenation of the strain parameters $\epsilon(\gamma,m)$ by the strain tensor ϵ_{ij} $(i,j=x,y,z)$ is obtained from the Kronecker product $\Gamma_4\otimes\Gamma_4$ using the symmetry of ϵ_{ij}.

$\epsilon(\gamma,m)$	ϵ_{ij}
$\epsilon(\Gamma_1)$	$\epsilon_{xx}+\epsilon_{yy}+\epsilon_{zz}$
$\epsilon(\Gamma_3,1)$	$2\epsilon_{zz}-\epsilon_{xx}-\epsilon_{yy}$
$\epsilon(\Gamma_3,2)$	$\sqrt{3}(\epsilon_{xx}-\epsilon_{yy})$
$\epsilon(\Gamma_5,1)$	ϵ_{yz}
$\epsilon(\Gamma_5,2)$	ϵ_{xz}
$\epsilon(\Gamma_5,3)$	ϵ_{xy}

TABLE IX. Bilinear forms $V_i(\gamma,\lambda)_m$. For V_1 the decomposition of $\Gamma_1\otimes\Gamma_1=\Gamma_1$ is used, for $V_5\Gamma_5\otimes\Gamma_5=\Gamma_1\oplus\Gamma_3(\oplus\Gamma_4)\oplus\Gamma_5$, and for $V_{15}\Gamma_1\otimes\Gamma_5=\Gamma_5$, where the components are excluded which cannot couple invariantly with the strain parameters. It has to be regarded that the $V_i(\gamma,\lambda)$ are real.

$V_i(\gamma,\lambda)_m$	λ_j
$V_i(\Gamma_1,\lambda)$	$\lvert\lambda_1\rvert^2$
$V_5(\Gamma_1,\lambda)$	$\lvert\lambda_7\rvert^2+\lvert\lambda_8\rvert^2+\lvert\lambda_9\rvert^2$
$V_5(\Gamma_3,\lambda)_1$	$2\lvert\lambda_9\rvert^2-\lvert\lambda_7\rvert^2-\lvert\lambda_8\rvert^2$
$V_5(\Gamma_3,\lambda)_2$	$\sqrt{3}(\lvert\lambda_7\rvert^2-\lvert\lambda_8\rvert^2)$
$V_5(\Gamma_5,\lambda)_1$	$\lambda_8^*\lambda_9+\lambda_8\lambda_9^*$
$V_5(\Gamma_5,\lambda)_2$	$\lambda_9^*\lambda_7+\lambda_9\lambda_7^*$
$V_5(\Gamma_5,\lambda)_3$	$\lambda_7^*\lambda_8+\lambda_7\lambda_8^*$
$V_{15}(\Gamma_5,\lambda)_1$	$e^{i\delta}\lambda_1\lambda_7^*+e^{-i\delta}\lambda_1^*\lambda_7$
$V_{15}(\Gamma_5,\lambda)_2$	$e^{i\delta}\lambda_1\lambda_8^*+e^{-i\delta}\lambda_1^*\lambda_8$
$V_{15}(\Gamma_5,\lambda)_3$	$e^{i\delta}\lambda_1\lambda_9^*+e^{-i\delta}\lambda_1^*\lambda_9$

$$(\lambda_1,\lambda_7,\lambda_8,\lambda_9)=(\lvert\lambda_1\rvert,\lvert\lambda\rvert e^{i\phi},0,0)$$

and $(\lvert\lambda_1\rvert,0,0,\lvert\lambda\rvert e^{i\phi})$, respectively, leading to a value

$$F_1-F_2=-6C_5(\Gamma_3)\epsilon_{zz}\lvert\lambda\rvert^2 . \quad (28)$$

There is a second type of domain wall in this CR phase separating domains

$$(\lvert\lambda_1\rvert,\pm\lvert\lambda\rvert e^{i\phi},0,0) .$$

In this case a [111] sound wave leads to a value

$$F_1-F_2=4C_{15}(\Gamma_5)\lvert\lambda_1\rvert\lvert\lambda\rvert\cos(\phi+\delta)\epsilon_{xy} . \quad (29)$$

Since both Eqs. (28) and (29) are different from zero in the CR phase, ultrasound is absorbed in both [001] and [111] direction in the low-temperature phase of the region II. A further result of this type of analysis is that the decomposition of $\Gamma\otimes\Gamma'$ has to contain the Γ_5 component in order to induce domain-wall motion by a longitudinal sound wave in the [111] direction. It turns out that the combinations (Γ_1,Γ_3) and (Γ_1,Γ_4) are not favorable from this point of view. On the other hand, either (Γ_3,Γ_4) or (Γ_3,Γ_5) are good combinations, and the same holds for (Γ_4,Γ_5).

IX. THE LOWER CRITICAL MAGNETIC FIELD

An interesting series of measurements on H_{c1}, the lower critical field, have been made by Rauchschwalbe *et al.*[16] We extend the GL expansion of the free energy by the addition of the magnetic field energy to consider this problem and also add gradient terms. A general expression for the gradient terms is given in Table X for the example (Γ_1,Γ_5), but to simplify the treatment we assume that the coefficients $K_1\approx K_2\approx K_3\approx K\neq 0$ and $K_4\approx K_5\approx K_6\approx 0$. The free energy F per unit volume in a magnetic field then has the form

$$F'=F+\frac{\mu_0}{2}H^2+K\sum_i \lvert\mathbf{D}\lambda_i\rvert^2 \quad i=1,7,8,9 , \quad (30)$$

TABLE X. General expression for gradient terms of (Γ_1,Γ_5).

Gradient terms	Coefficients
$\lvert D_x\lambda_1\rvert^2+\lvert D_y\lambda_1\rvert^2+\lvert D_z\lambda_1\rvert^2$	K_1
$\lvert D_x\lambda_7\rvert^2+\lvert D_y\lambda_8\rvert^2+\lvert D_z\lambda_9\rvert^2$	K_2
$\lvert D_y\lambda_7\rvert^2+\lvert D_z\lambda_7\rvert^2+\lvert D_x\lambda_8\rvert^2+\lvert D_z\lambda_8\rvert^2+\lvert D_x\lambda_9\rvert^2+\lvert D_y\lambda_9\rvert^2$	K_3
$(D_x\lambda_7)^*(D_y\lambda_8)+(D_z\lambda_9)^*(D_x\lambda_7)+(D_y\lambda_8)^*(D_z\lambda_9)+\text{c.c.}$	K_4
$(D_z\lambda_8)^*(D_y\lambda_9)+(D_z\lambda_7)^*(D_x\lambda_9)+(D_y\lambda_7)^*(D_x\lambda_8)+\text{c.c.}$	K_5
$(D_x\lambda_1)^*(D_9\lambda_9+D_z\lambda_8)+(D_y\lambda_1)^*(D_x\lambda_9+D_z\lambda_7)+(D_z\lambda_1)^*(D_x\lambda_8+D_y\lambda_7)+\text{c.c.}$	K_6

where μ_0 denotes the magnetic permeability and $\mathbf{D}=\hbar/i\nabla-2e\,\mathbf{A}$ ($\mathbf{A}$: vector potential, e: elementrary charge). The variation of Eq. (30) with respect to $\mathbf{A}$ leads to the following expression for the supercurrent, neglecting spatial inhomogeneities of the order parameter, i.e., we are neither near the material surface nor a domain wall,

$$\mathbf{J}=-4e^2\mu_0K\,\mathbf{A}\sum_i|\lambda_i|^2=-\frac{1}{\delta^2}\mathbf{A}\ , \tag{31}$$

and δ is the London penetration depth. The thermodynamic critical field $H_c(T)$ is derived from the equilibrium condition

$$F(T)=-\frac{\mu_0}{2}H_c^2(T)\ . \tag{32}$$

In a type II superconductor, the lower and upper critical fields are related to H_c by the Abrikosov or GL parameter κ in the limit $\kappa\gg 1$,

$$H_{c1}=H_c(T)\frac{\ln\kappa}{\kappa\sqrt{2}}\ ,\qquad H_{c2}=H_c(T)\kappa\sqrt{2}\ , \tag{33}$$

and κ is defined by

$$\kappa=2\sqrt{2}\frac{\mu_0 e}{\hbar}H_c(T)\delta^2(T)\ . \tag{34}$$

In contrast to the effective quadratic temperature dependence of $H_c(T)(=H_c(0)[1-(T/T_c)^2]$, in GL theory Eqs. (32) and (34) lead to linear behavior, which is only a good approximation for T near T_c. Nevertheless, we may consider the qualitative properties of the lower critical field in the region II, especially near the second transition.

We consider now the simplest case corresponding to Fig. 3(a). In the SR phase with Γ_1, the thermodynamical field and the GL parameter are given by

$$H_c^{(\mathrm{SR})}(T)=A_1(T)\sqrt{\alpha/3\mu_0\beta}\ ,\qquad \kappa_{\mathrm{SR}}(T)=\frac{1}{K\hbar e}\sqrt{2\alpha\beta/3\mu_0}\ , \tag{35}$$

and in the lower-temperature CR phase the corresponding formulas are

$$H_c^{(\mathrm{CR})}(T)=(4\alpha[(\eta_1'+\eta_2')A_1^2+\beta A_5^2-QA_1A_5]/\{3\mu_0[4\beta(\eta_1'+\eta_2')-Q^2]\})^{1/2}\ ,$$
$$\kappa_{\mathrm{CR}}(T)=\frac{1}{K\hbar e}\sqrt{2\alpha/3\mu_0}\{[4\beta(\eta_1'+\eta_2')-Q^2][(\eta_1'+\eta_2')A_1^2+\beta A_5^2-QA_1A_5]\}^{1/2}/[Q(A_1+A_5)-2(\eta_1'+\eta_2')A_1-2\beta A_5]\ , \tag{36}$$

derived using the Eqs. (12), (14), (15), (32), and (34).

$$\alpha\approx 10^{-23}T_c^2 JK^{-2}m^{-3}$$

if we take F as the free energy per unit volume. With the values for the parameters β, $(\eta_1'+\eta_2')$ and Q obtained from the specific heat data for $x=0.033$, we plot κ and the lower critical field $B_{c1}=\mu_0H_{c1}$ in Fig. 6. The qualitative behavior of the critical field is well described. $B_{c1}(T)$ has a sharp kink at the second transition temperature at which the slope increases strongly, caused by the increase of the condensation energy of the superconducting state at this transition. This property agrees with the measurements of B_{c1} by Rauchschwalbe *et al.* From their data we estimate that the coefficient K^{-1} has a value of about $17\,m_e$ m^3 (m_e: electron mass).

X. MAGNETIC PROPERTIES AND μSR EXPERIMENTS

Volovik and Gor'kov[6] pointed out that the violation of time reversal by nonunitary states (i.e., states with $\mathbf{d}^*\neq\mathbf{d}$ or $\psi^*\neq\psi$) implies a certain magnetic property of the corresponding superconducting phase. Since superconductivity and a bulk magnetic moment are incompatible (i.e., $\mathbf{B}=\mathbf{0}$), screening supercurrents will occur in a small range ($\sim\delta$) near the domain walls and surfaces, even if no external magnetic field is present.

However, we are interested, in this section, in the response to muons and therefore in the local magnetic moment at the muon position. The spin operator at a position $\mathbf{r}$ is

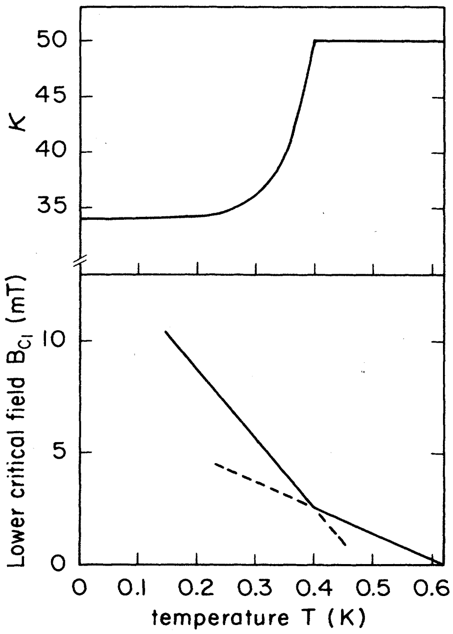

FIG. 6. GL parameter and the lower critical magnetic field. The data derived in Sec. VII are used to plot this function of temperature at the Th concentration $x=0.033$, where we set the parameter $K\approx 17\,m_e\ \mathrm{m}^3$. (a) The GL parameter changes continuously from $\kappa\approx 50$ to ≈ 35 below the transition temperature $T=0.4$ K. The discontinuity in the first derivative is also found in the lower critical magnetic field (b) $B_{c1}=\mu_0 H_{c_1}$. The enhancement of the B_{c_1} points to an increase of the condensation energy below 0.4 K.

$$\begin{aligned}\hat{\mathbf{S}}(\mathbf{r})&=\sum_{\gamma,\delta}\Psi^\dagger_\gamma(\mathbf{r})\hat{\mathbf{S}}\Psi_\delta(\mathbf{r})\\ &=\frac{\hbar}{2}\sum_{\substack{\mathbf{k},\mathbf{k}'\\ s,s',\gamma,\delta}}\chi^*_{\mathbf{k},\gamma s}(\mathbf{r})\boldsymbol{\sigma}_{ss'}\chi_{\mathbf{k}',\delta s'}(\mathbf{r})e^{i(\mathbf{k}'-\mathbf{k})\cdot\mathbf{r}}c^\dagger_{\mathbf{k}\gamma}c_{\mathbf{k}'\delta}\ ,\end{aligned}\tag{37}$$

where the field operator $\Psi^\dagger_\gamma(\mathbf{r})$ is expanded in Bloch states which are not eigenstates of spin because of spin orbit coupling:

$$\Psi^\dagger_\gamma(\mathbf{r})=\sum_{\mathbf{k}}[\chi_{\mathbf{k},\gamma\uparrow}(\mathbf{r})|\uparrow\rangle+\chi_{\mathbf{k},\gamma\downarrow}(\mathbf{r})|\downarrow\rangle]e^{i\mathbf{k}\cdot\mathbf{r}}c^\dagger_{\mathbf{k}\gamma}\ .\tag{38}$$

$\chi_{\mathbf{k},\gamma\uparrow}(\mathbf{r})$ denotes the spin-up component of the Bloch function with wave vector $\mathbf{k}$ and pseudospin index γ. The indices γ and δ label the spinor states which are obtained from the spin eigenstates by an adiabatic turn on of the spin orbit interaction. The operator $c_{\mathbf{k}\gamma}$ ($c^\dagger_{\mathbf{k}\gamma}$) is the annihilation (creation) operator of the Bloch spinor state $|\mathbf{k},\gamma\rangle$ and $\boldsymbol{\sigma}=(\sigma^x,\sigma^y,\sigma^z)$ are the Pauli spin matrices. The superconducting ground state can be written in a BCS form

$$|\Phi\rangle=\prod_{\mathbf{k},\alpha}\sum_{\beta}(u_{\mathbf{k},\alpha\beta}+v_{\mathbf{k},\alpha\beta}c^\dagger_{\mathbf{k}\alpha}c^\dagger_{-\mathbf{k}\beta})|0\rangle\ ,\tag{39}$$

where we restrict the product over $\mathbf{k}$ to a half space. For $u_{\mathbf{k},\alpha\beta}$ and $v_{\mathbf{k},\alpha\beta}$ we use the convenient form which is a reasonable approximation near the second transition:

$$\begin{aligned}u_{\mathbf{k},\alpha\beta}&=\frac{(E_{\mathbf{k}}+\epsilon_{\mathbf{k}})\delta_{\alpha\beta}}{[\frac{1}{2}\mathrm{tr}(\Delta^\dagger\Delta)+(E_{\mathbf{k}}+\epsilon_{\mathbf{k}})^2]^{1/2}}\ ,\\ v_{\mathbf{k},\alpha\beta}&=\frac{\Delta_{\alpha\beta}(\mathbf{k})}{[\frac{1}{2}\mathrm{tr}(\Delta^\dagger\Delta)+(E_{\mathbf{k}}+\epsilon_{\mathbf{k}})^2]^{1/2}}\ .\end{aligned}\tag{40}$$

$\Delta_{\alpha\beta}(\mathbf{k})$ is the matrix defined in Eq. (1) and

$$E_{\mathbf{k}}=[\epsilon^2_{\mathbf{k}}+\tfrac{1}{2}\mathrm{tr}(\Delta^\dagger\Delta)]^{1/2}\ .$$

Cooper pairing is only possible between Bloch states which are degenerate by parity, time reversal or their product as mentioned in Ref. 7.

It is a long, but straightforward calculation to show that for a spin triplet pairing state the expectation value of the spin operator has the form

$$S_\mu(\mathbf{r})=\langle\Phi|\hat{S}_\mu(\mathbf{r})|\Phi\rangle=\sum_{\mathbf{k},\nu}g_{\mu\nu}(\mathbf{k},\mathbf{r})S_\nu(\mathbf{k})\ ,\tag{41}$$

with

$$\mathbf{S}(\mathbf{k})=\frac{4\hbar}{i}\frac{\mathbf{d}^*(\mathbf{k})\times\mathbf{d}(\mathbf{k})}{N(\mathbf{k})}\ ,\tag{42}$$

where $N(\mathbf{k})=\frac{1}{2}\mathrm{tr}(\Delta^\dagger\Delta)+(E_{\mathbf{k}}+\epsilon_{\mathbf{k}})^2$. $g_{\mu\nu}(\mathbf{k},\mathbf{r})$ is the g tensor which takes the effect of the spin-orbit coupling into account and is formed from the Bloch functions $\chi_{\mathbf{k}\gamma s}(\mathbf{r})$ in Eq. (38):

$$g_{\mu\nu}(\mathbf{k},\mathbf{r})=\frac{1}{2}\sum_{\substack{s,s'\\ \gamma,\delta}}\sigma^\mu_{ss'}\sigma^\nu_{\gamma\delta}\chi^*_{\mathbf{k},\gamma s}(\mathbf{r})\chi_{\mathbf{k},\delta,s'}(\mathbf{r})\ ,\tag{43}$$

where $\sigma^\mu_{ss'}$ denotes the μth Pauli spin matrix. This ensures that $g_{\mu\nu}(\mathbf{k},\mathbf{r})$ is periodic in space with the lattice constant and has the whole symmetry of the little group of $\mathbf{k}$ of the crystal lattice in $\mathbf{r}$ space and vice versa. Therefore, $\mathbf{S}(\mathbf{r})$ describes a spin-density wave with the period of the lattice. Certain information about the $\mathbf{r}$ dependence of $\mathbf{S}$ can be obtained by symmetry arguments, if we note that for each point group element R,

$$S_\mu(R\mathbf{r})=\sum_{\mathbf{k},\nu}g_{\mu\nu}(\mathbf{k},\mathbf{r})S_\nu(R\mathbf{k})\ ,\tag{44}$$

where we use the property that

$$g_{\mu\nu}(\mathbf{k},R\mathbf{r})=g_{\mu\nu}(R^{-1}\mathbf{k},\mathbf{r})$$

obtained from

$$\chi_{\mathbf{k}}(R\mathbf{r})=\chi_{R^{-1}\mathbf{k}}(\mathbf{r})\ .$$

A nonunitary state $\mathbf{d}(\mathbf{k})$ generates a finite local spin polarization in each unit cell of the lattice. Note that such a local polarization is fully compatible with the condition $\mathbf{B}=0$ in the bulk superconductor, since the spatial average of $\mathbf{S}(\mathbf{r})$ in each unit cell vanishes leading to no total magnetic moment. This is easy to derive from Eq. (44). For spin singlet states, however, similar calculations lead to a vanishing local spin density everywhere in the unit cell.

Recently, Heffner *et al.* have observed in their μSR experiments a significant, rather abrupt increase of the zero-field relaxation rate, Λ, of positive muons injected in $U_{1-x}Th_xBe_{13}$ with $x=0.033$ at the second transition temperature.[17] Λ is a measure for a local static, random magnetic field spread in the sample.[24] If a simple hyperfine contact interaction between the conduction electron and the muon spin is assumed, the magnetic field felt by the muon is directly proportional to the spin polarization at the muon site. Therefore we can approximately set the relaxation rate

$$\Lambda \propto \sqrt{\Delta s^2} = \left[\sum_i \int d^3r\, \delta(\mathbf{r}-\mathbf{r}_i)\mathbf{S}^2(\mathbf{r}) \right]^{1/2} , \tag{45}$$

where the integral ranges over a unit cell and $\mathbf{r}_i$ are the trapping points of a muon in the unit cell. In general, they are at crystallographic equivalent points with a certain symmetry environment of neighboring atoms.[24] However, a zero-field relaxation rate can only be observed if the magnitude and the direction of the spin polarization varies randomly among the trapping points (i.e., there are not only a few favored directions and magnitudes of the magnetic field at the trapping points). For a pure crystal of UBe_{13}, where these trapping points should lie regularly in the unit cell, this condition may not be satisfied, since only different directions and not magnitudes of the spin polarization may occur at these points. This is easily seen from Eq. (44). However, in alloys with finite Th concentrations, the trapping points have a more irregular distribution because of local violations of the lattice symmetry. We take this distribution into account by replacing $\delta(\mathbf{r}-\mathbf{r}_i)$ by a function $d(\mathbf{r}-\mathbf{r}_i)$ which smears out the trapping points around $\mathbf{r}_i$ as an average over all unit cells. In this case the muons experience a real spread of the spin polarization.

In region II the superconducting state of the low-temperature phase is indeed generally the CR phase and therefore always nonunitary, whereas the high-temperature phase may be a unitary state. In this case no increase in the zero-field relaxation rate occurs at the onset of superconductivity, but it is expected at the second transition. For our simplest example

$$\mathbf{d}(\mathbf{k}) = \frac{|\lambda_1|}{\sqrt{3}}(\hat{\mathbf{x}}k_x + \hat{\mathbf{y}}k_y + \hat{\mathbf{z}}k_z) + e^{i\gamma_2}\frac{|\lambda_7|}{\sqrt{2}}(\hat{\mathbf{y}}k_z + \hat{\mathbf{z}}k_y) ,$$

(see Table IV) the variance of the spin polarization $(\Delta S^2)^{1/2}$ has a steep increase at the second transition temperature T_{c2}. At still lower temperature $(\Delta S^2)^{1/2}$ becomes constant. Since

$$\Lambda \propto (\Delta S^2)^{1/2} \propto |\lambda_1||\lambda_7| \tag{46}$$

the qualitative behavior of $\Lambda(T)$ can easily be calculated. For $|\lambda_1|^2$ and $|\lambda_7|^2$ we use the result (15) and the behavior of $\Lambda(T)$ is shown in Fig. 7. This temperature dependence is in good qualitative agreement with with Heffner *et al.* measurements.[17] On the other hand, no change of

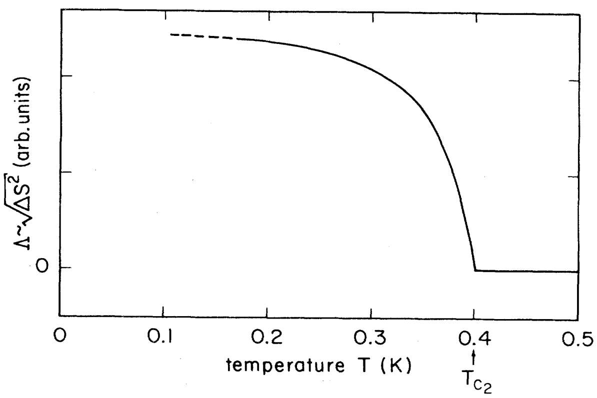

FIG. 7. The zero-field relaxation rate Λ. The temperature dependence of Λ is proportional to $\Delta S^2(T)$. We picture Eq. (46) with arbitrary units using the data of $x=3.3\%$ where $T^{(0)}=0.4$ K. The sharp increase of Λ is qualitatively in a good agreement with Heffner's observation (Ref. 17).

Λ is observed in pure UBe_{13} at the transition temperature. At present, we have no measurements for a finite Th concentration in the region I in order to decide whether the superconducting state is unitary or nonunitary there.

XI. CONCLUSION

We have shown that the proposal of two different types of superconductivity in the two regions yields good qualitative descriptions of many experimental factors. As mentioned, we treated here only the simplest examples among many other possible cases. Nevertheless, some general results can be given. The most important point is that generally the low-temperature phase of the region II is *nonunitary,* i.e., it possesses magnetic properties as pointed out by Volovik and Gor'kov.[6] In the case of spin triplet pairing this leads to a spin-density wave. In Sec. X it was shown that this fact influences μSR zero-field relaxation rate data. Further measurements of this type in region I could give information as to whether the superconducting phase has similar magnetic properties there or not. Since this low-temperature phase in our model is a CR superconducting state which belongs to a combination of two irreducible representations $\Gamma \oplus \Gamma'$, the condensation energy is enhanced at its onset compared wtih the SR phase. This fact is confirmed by experimental data of the critical magnetic field. The low symmetry of this CR phase will cause additional ultrasonic attenuation induced by domain-wall motion for all directions of the sound wave. Thus, we believe we have achieved a complete and consistent explanation of all the experimental data to date on the phase diagram of $U_{1-x}Th_xBe_{13}$, at least on a phenomenological level.

Very recently, Kumar and Wolfle investigated a similar theory in an isotropic model based on a crossing of s- and d-wave superconductivity at x_0 (in region I d wave and in region II s wave superconductivity is relevant).[21] With this proposal they found a possibility of two consecutive second-order transitions ($n \rightarrow s$ wave$\rightarrow s+d$ wave). In their calculations the lower critical field also increases as an effect of the increase of superconducting condensation energy at the second transition temperature. The ultrasonic attentuation peak is related to a collective mode arising from the dynamics of the relative phase angle of the combined phase. Their heuristic argument for the suppression of the d-wave state and the preference for the s-wave state with enhancement of the Th concentration could also be applied to our simplest example (Γ_1, Γ_5): the anisotropic Γ_5 states are strongly affected by impurity scattering (Th impurities), whereas the fully symmetric Γ_1-pairing state remain more or less unchanged.

Note Added in Proof. Recently, we investigated the domain wall mechanism (Sec. VIII) in more detail. Under the assumption that this mechanism is relevant for the ultrasound absorption in region II we could further restrict the number of possible combinations (Γ, Γ') outlined in Sec. VIII. In this analysis (Γ_1, Γ_5), as discussed in Sec. IV B with the phase diagram in Fig. 3, leads to the most favorable model. Details of this investigation will be published elsewhere.

ACKNOWLEDGMENTS

We thank R. Joynt, Chr. Bruder, A. Schenk, R. H. Heffner, and H. R. Ott for informative discussion and advice. We are also grateful to the Swiss National Foundation for financial support.

APPENDIX

We mentioned in Sec. IV A that under special conditions the θ_3 term allows a continuous transition between the SR phase of Γ_1 and the CR phase $(T_1 > T_3)$. For this to occur the coupling terms must have the effective form $\sim|\lambda_1|^2|\lambda|^2$ or $|\lambda|^4$. In Eq. (12) we have a CR state with fixed angle $\psi=\pi/4$ and $\phi_2+\phi_3=\pi$, neglecting the θ_3 coupling term. These values lead to $Q_3=0$ [Eq. (10)]. For fintie $\theta_3(<\theta_2)$, however, the angle ψ is no longer a fixed quantity, but deviates smoothly from $\pi/4$ below $T_1^{(0)}$. Therefore, near $T_1^{(0)}$ we set

$$\psi=\pi/4+\epsilon, \quad 0<\epsilon\ll 1(\theta_3>0)\ ;$$

$\phi_2+\phi_3=\pi$ we keep fixed $(\phi_2=\pi,\ \phi_3=0)$:

$$Q_3=\theta_3\sin(2\psi)(\cos\psi-\sin\psi)$$
$$=-\theta_3\sqrt{2}\sin\epsilon\approx-\theta_3\sqrt{2}\,\epsilon\ .$$

To obtain ϵ we minimize f of Eq. (10) with respect to ψ,

$$0=[2\beta_2|\lambda|^4\sin(2\psi)-\theta_2|\lambda_1|^2|\lambda|^2]\cos(2\psi)-\theta_3|\lambda_1||\lambda|^3[(\cos\psi-\sin\psi)\cos(2\psi)+\tfrac{1}{2}(\cos\psi+\sin\psi)\sin(2\psi)]\ .$$

Since ψ is not determined for $|\lambda|=0$, we assume $0<|\lambda|\ll|\lambda_1|$ near $T_1^{(0)}$. With $\cos(2\psi)\approx\epsilon$ and $\sin(2\psi)\approx 1$, we obtain an equation in ϵ:

$$\epsilon^2 2\sqrt{2}\theta_3|\lambda_1||\lambda|+\epsilon(4\beta_2|\lambda|^2-2\theta_2|\lambda_1|^2)+\frac{\theta_3}{\sqrt{2}}|\lambda_1||\lambda|=0\ .$$

An expansion of ϵ to lowest order in the small ratio $|\lambda|/|\lambda_1|$ leads to

$$\epsilon\approx\frac{\theta_3}{2\sqrt{2}\theta_2}\frac{|\lambda|}{|\lambda_1|}>0\ .$$

Higher-order terms contains ratios $\sim(|\lambda|/|\lambda_1|)^{2n+1}$ (n: integer). The θ_3 term then has the effective form

$$Q_3|\lambda_1||\lambda|^3\rightarrow-\sqrt{2}\frac{\theta_3^2}{2\sqrt{2}\theta_2}|\lambda|^4 \quad \text{for}(T-T_1^{(0)})\rightarrow 0-\ ,$$

and therefore it favors a continuous transition at $T_1^{(0)}$. In the case $T_3>T_1$, the SR phase immediately below T_3 has, for example, the form $\lambda_2'\neq 0$, $\lambda_1=\lambda_3'=0$ [Eq. (11c)], i.e., $\psi=0$. We consider f for $\psi\rightarrow 0$ and $|\lambda_1|\rightarrow 0$ and minimize with respect to ψ.

$$\frac{\partial f}{\partial\psi}=4\beta_2|\lambda|^4\psi+\theta_2C_1|\lambda|^2|\lambda_1|^2$$
$$+\theta_3C_2|\lambda|^3|\lambda_1|+3\theta_3C_3|\lambda|^3|\lambda_1|\psi=0\ ,$$

where

$$C_1=\cos(2\phi_1-\phi_2-\phi_3-\gamma_2)\ ,$$

$$C_2=\cos(\phi_1+\phi_3-2\phi_2-\gamma_3)\ ,$$

and

$$C_3=\cos(\phi_1+\phi_2-2\phi_3-\gamma_3)\ .$$

We solve this equation for ψ using $|\lambda_1|\rightarrow 0$.

$$\psi\approx-\frac{\theta_3C_2|\lambda_1|}{4\beta_2|\lambda|}+\left[\frac{3\theta_3^2C_2}{(4\beta_2)^2}-\frac{\theta_2C_1}{4\beta_2}\right]\frac{|\lambda_1|^2}{|\lambda|^2}\ .$$

If we insert this solution in f with the same approximation, we obtain the following significant term:

$$\frac{3\theta_3^3C_2^2}{(4\beta_2)^2}|\lambda_1|^3|\lambda|\ ,$$

which is responsible to a first-order transition instability, since it is a "quasi-third-order term" as seen in Sec. IV. Therefore, this case can be neglected in point of view of explaining the phase diagram under consideration.

[1]F. Steglich, J. Aarts, C. D. Brendl, W. Lieke, D. Meschede, W. Franz, and J. Schäfer, Phys. Rev. Lett. **43**, 1892 (1979).

[2]H. R. Ott, H. Rudigier, Z. Fisk, and J. L. Smith, Phys. Rev. Lett. **50**, 1595 (1983).

[3]G. R. Stewart, Z. Fisk, J. O. Willis, and J. L. Smith, Phys. Rev. Lett. **52**, 679 (1984).

[4]H. R. Ott, Helv. Phys. Acta **60**, 62 (1987).

[5]D. Rainer, Phys. Scr. **T23**, 106 (1988).

[6]G. E. Volovik and L. P. Gor'kov, Zh. Eksp. Teor. Fiz. **39**, 550 (1984) [Sov. Phys.—JETP **39**, 674 (1984)]; **88**, 1412 (1985) **61**, 843 (1985)].

[7]U. Ueda and T. M. Rice, Phys. Rev. B **31**, 7114 (1985).

[8]E. I. Blount, Phys. Rev. B **32**, 2935 (1985).

[9]M. Ozaki, K. Machida, and T. Ohmi, Prog. Theor. Phys. **74**, 221 (1985); Prog. Theor. Phys. **75**, 442 (1986).

[10]H. Monien, K. Scharnberg, L. Tewordt, and N. Schopohl, Phys. Rev. B **34**, 3487 (1986); J. Low Temp. Phys. **65**, 13 (1986).

[11]J. L. Smth, Z. Fisk, J. O. Willis, B. Batlogg, and H. R. Ott, J. Appl. Phys. **55**, 1996 (1984).

[12]H. R. Ott, H. Rudigier, Z. Fisk, and J. L. Smth, Phys. Rev. B **31**, 1651 (1985).

[13]B. Batlogg, D. Bishop, B. Golding, C. M. Varma, Z. Fisk, J. L. Smith, and H. R. Ott, Phys. Rev. Lett. **55**, 1319 (1985).

[14]D. Bishop, B. Batlogg, B. Golding, Z. Fisk, and J. L. Smith, Phys. Rev. Lett. **57**, 2095 (1986).

[15]S. E. Lambert, Y. Dalichaoud, M. B. Maple, J. L. Smith, and Z. Fisk, Phys. Rev. Lett. **57**, 1619 (1986).

[16]U. Rauchschwalbe, F. Steglich, G. R. Stewart, A. L. Giorgi, P. Fulde, and K. Maki, Europhys. Lett. **3**, 751 (1987).

[17]R. H. Heffner, D. W. Cooke, and D. E. MacLaughlin, in *Theoretical and Experimental Aspects of Valence Fluctuations and Heavy Fermions,* edited by L. C. Gupta and S. K. Malik (Plenum, New York, 1987).

[18]R. Joynt, T. M. Rice, and K. Ueda, Phys. Rev. Lett. **56**, 1412 (1986).

[19]K. Machida and M. Kato, Phys. Rev. Lett. **58**, 1986 (1987).

[20]U. Rauchschwalbe, C. D. Bredl, F. Steglich, K. Maki, and P. Fulde, Europhys. Lett. **3**, 757 (1987).

[21]P. Kumar and P. Wölfle, Phys. Rev. Lett. **59**, 1954 (1987).

[22]M. Sigrist, R. Joynt, and T. M. Rice, Europhys. Lett. **3**, 629 (1987); Phys. Rev. B **36**, 5186 (1987).

[23]J. Keller, K. Scharnberg, and H. Monien, Physica C **152**, 302 (1988).

[24]A. Schenk, *Muon Spin Rotation Spectroscopy* (Hilger, London, 1985).